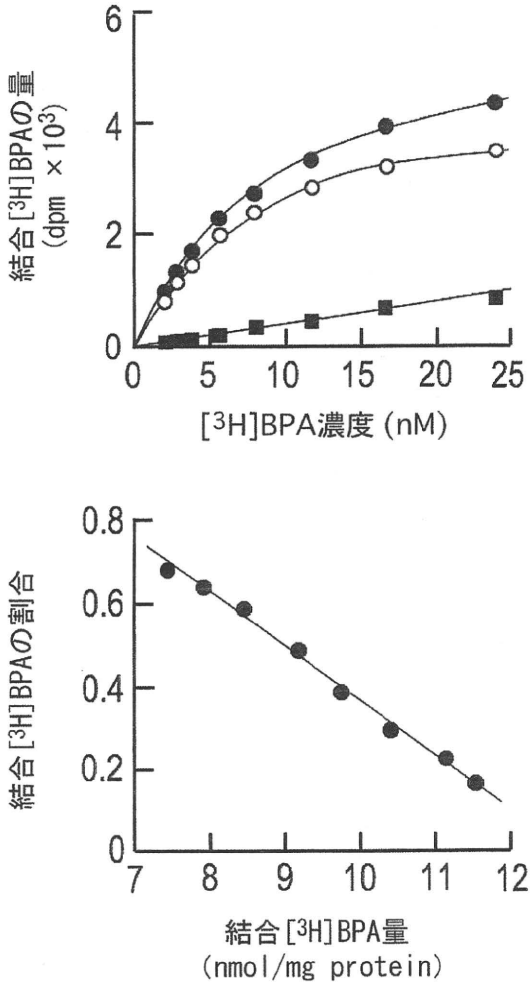

図1　[³H]BPAによるERRγ飽和結合試験の結果
(上) ●：全結合，○：特異的結合，■：非特異的結合を示す。縦軸は，結合した[³H]BPAの壊変数，横軸は，使用した[³H]BPAの濃度を示す。(下)スキャッチャードプロット解析の結果を示す。縦軸は遊離の[³H]BPAに対する結合した[³H]BPAの比率，横軸は単位蛋白質量あたりに結合した[³H]BPAを示す。線形グラフは直線で，結合部位が一つであることを示し，その傾きは$-1/K_D$である。また，X切片がB_{max}値を示し，これは蛋白質1 mgあたりの最大結合量を意味する。(文献7より改変して引用) なお，結合部位の数についてはX線結晶解析より証明された[8),9)]

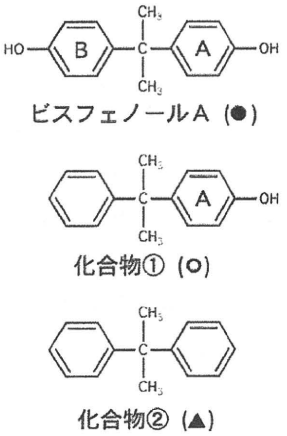

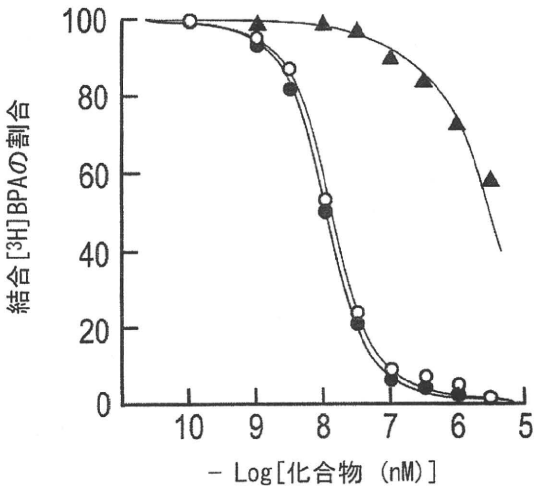

図2　[³H]BPAによるERRγ競争結合試験の結果
ビスフェノールA，化合物①及び化合物②について，[³H]BPAの結合に対する阻害能を解析した。これにより，調べたい化合物の結合性を相対的に評価することができる。縦軸は化合物を競合させていないときの[³H]BPA結合数と競合後の[³H]BPA結合数の割合を百分率で示す。横軸は競合させた化合物濃度を示す。BPAと化合物①はフェノール環Aを共有し，これらはERRγの同じ部位に結合する[9)]

スフェノールAと比較する。これにより，一つのOH基がきわめて重要であることがわかる（図2)。こうした解析を網羅的に行い，ビスフェノール類とアルキルフェノール類がERRγに強く結合することを明らかにした[7)]。更に，筆者らは，ビスフェノールAが結合したERRγの結晶構造解析にも成功し[8),9)]，もはや，ビスフェノールAやその類似体のERRγ結合性は疑いようがない。

一方，ビスフェノールAによるERRγの活性変化を調べたところ，驚きの結果が得られた。

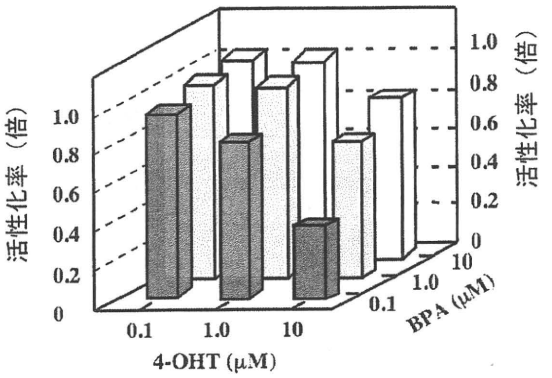

図3 インバースアンタゴニスト活性の測定結果
レポーター遺伝子アッセイでERRγの活性を測定した結果を示す。縦軸は活性の大きさ，横軸はリガンド濃度を示す。4-OHTによりERRγの自発活性が減少するが，ビスフェノールAを加えることで活性が回復した（インバースアンタゴニスト活性）。インバースアンタゴニストは，濃度依存的に作用した。（文献4より改変して引用）

ビスフェノールAは，ERRγに強力に結合するが，ERRγの自発活性に対して何の影響も示さなかった。更に，4-OHTと競合させた場合，4-OHTのインバースアゴニスト活性を顕著に阻害した（図3）。つまり，ビスフェノールAはERRγの「インバースアンタゴニスト」であることが判明した[4),5),7)]。インバースアンタゴニスト活性はこれまでにない概念であり，生理学的な意義については不明である。したがって，現在のところ，ビスフェノールAによる生体への影響，分子機構は想像もつかない。ビスフェノールAの内分泌かく乱作用にERRγが関与しているのか？を含めて，新しい研究視点で世界中の研究機関で解析が始まっている。近い将来，ビスフェノールA問題の全容が明らかにされるものと期待される。

6. おわりに

「受容体科学」の分野では，近年，分子間相互作用を様々な原理に基づく測定から解析しようとする流れがある。BIAcore，SPR，QCM，等々。しかし，筆者らの経験からすると，「受容体に強く結合する化合物を放射標識したものをリガンドとして解析し，これをトレーサとした競争結合試験で結合の構造要因を探り，更に強く結合する化合物を探索し，あるいは分子デザインする」こうした一連の解析に勝るものはないように思われる。受容体結合試験。高価であるが，結果も高価値である。ビスフェノールAのトリチウム標識体は，このように受容体結合試験に活躍できるとは夢にも思っていなかったに違いない。しかし，今，この放射標識化合物こそが，最もホットな化合物なのである。

文 献

1) NTP BRIEF ON BISPHENOL A (Peer Review Date : June 11, 2008) National Toxicology Program (National Institute of Environmental Health Sciences, NIH, US-HHS)
2) http : // www.rsc.org/chemistryworld/Issues/2008/April/Bis phenolABabyBottleDebate. asp
3) Welshons, W. V., Nagel, S. C. et al., *Endocrinology*, **147**, S56-S69 (2006)
4) Takayanagi, S., Tokunaga, T. et al., *Toxicol. Lett.*, **167**, 95-105 (2006)
5) Liu, X., Matsushima, A. et al., *FEBS J.*, **274**, 6340-6351 (2007)
6) Coward, P., Lee, D. et al., *Proc. Natl. Acad. Sci.*, **98**, 8880-8884 (2001)
7) Okada, H., Tokunaga, T. et al., *Environ. Health Perspect.*, **116**, 32-38 (2008)
8) Matsushima, A., Kakuta, Y. et al., *J. Biochem.*, **142**, 517-524 (2007)
9) Matsushima, A., Teramoto, T. et al., *Biochem. Biophys. Res. Commun.*, **373**, 408-413 (2008)

Toxicology Letters 191 (2009) 33–39

Contents lists available at ScienceDirect

Toxicology Letters

journal homepage: www.elsevier.com/locate/toxlet

Exploration of endocrine-disrupting chemicals on estrogen receptor α by the agonist/antagonist differential-docking screening (AADS) method: 4-(1-Adamantyl)phenol as a potent endocrine disruptor candidate

Takeru Nose*, Takatoshi Tokunaga, Yasuyuki Shimohigashi

Laboratory of Structure-Function Biochemistry, Department of Chemistry, Faculty of Sciences, Kyushu University, 6-10-1 Hakozaki, Higashi-ku, Fukuoka 812-8581, Japan

ARTICLE INFO

Article history:
Received 4 April 2009
Received in revised form 31 July 2009
Accepted 4 August 2009
Available online 8 August 2009

Keywords:
Endocrine disruptor
Estrogen receptor α
Docking calculation

ABSTRACT

We established a novel screening method to survey endocrine-disrupting chemicals by means of *in silico* docking calculations. Endocrine disruptors target the human nuclear receptor, which bind a chemical in a pocket presenting in the ligand-binding domain (LBD). The LBD alters its conformation, depending upon the binding of either agonist or antagonist. We discovered that the chemicals can be differentiated into either agonist or antagonist by the docking calculations of the chemical for the LBD. We used the crystal structures of both agonist-bound LBDs and antagonist-bond LBDs as templates in the docking calculations, and estimated binding energies to discriminate between agonist and antagonist bindings. This agonist/antagonist differential-docking screening (AADS) method predicted, for example, 4-(1-adamantyl)phenol as an agonist of the human estrogen receptor α (hERα). Indeed, this compound, one of the essential raw materials for nanoporous organosilicate thin films, was confirmed to exhibit strong agonist activity in the reporter-gene assay for hERα with a high binding affinity. The AADS method is an approach that appears to foresee both the binding ability and the agonist/antagonist function of chemicals for the target nuclear receptors.

1. Introduction

Nuclear receptors (NRs) play a central role as transcription factors in biological processes such as cell growth and differentiation, embryonic development, and metabolic homeostasis in metazoan organisms. Most of these NRs directly activate target genes by binding to the DNA response elements in conjunction with the hormone binding specific to the NR's ligand-binding domain (LBD). Mostly, NR-LBDs possess a pocket that is able to capture a hormone or a hormone-like chemical to build up the activation conformation (Germain et al., 2006; Heldring et al., 2007; Olefsky, 2001), while the antagonist disrupts this conformation so that the NR cannot bind the coactivator proteins. This conformation preference or discrimination by a specific agonist/antagonist is a common molecular recognition mechanism of most NRs.

The conformational difference between the agonist-bound LBD and antagonist-bound LBD is primarily described by different positioning of the α-helix No. 12 in the NR-activation function 2 (AF2) in the C-terminal region of LBD (Brzozowski et al., 1997; Shiau et al., 1998). In the activation conformation, the AF-2-α-helix is positioned so that it covers up the ligand-binding pocket (LBP), where the ligand, and especially the agonist, usually docks. By contrast, the antagonist rejects the AF-2-α-helix binding and it pushes away the helix in other locations. It should be noted that this discrimination is definitely due to the molecular size of the antagonist being much larger than that of the agonist. This size difference substantiates the discrepancy between the volumes of agonist-bound LBP and the antagonist-bound LBP, providing different molecular surface reactants necessary for ligand–receptor interactions.

If we could forecast the compounds that would fit into the LBP, it would definitely be advantageous for the design of agonist or antagonist ligands of particular NR. It would also be very helpful to predict which chemicals would bind to NRs and as a result cause serious disruptions in the endocrine system. Knowledge of the structures of agonist-bound and antagonist-bound LBP is certainly beneficial in making these structural predictions, and computational analysis is a powerful methodology for obtaining such knowledge. In fact, there have been many reports of screening procedures for identification of endocrine-disrupting chemicals (Celik et al., 2008; Cui et al., 2009; Fukuzawa et al., 2003, 2005; Hong et al., 2002; István Virága et al., 2005; Nose and Shimohigashi, 2008; Schmieder et al., 2003; Selassie et al., 2003). However, the calcula-

Abbreviations: AADS, the agonist/antagonist differential-docking screening; AF2, activation function 2; *Cpf*, conformation preference factor; EDC, endocrine-disrupting chemical; ERα, estrogen receptor α; LBD, ligand-binding domain; LBP, ligand-binding pocket; NR, nuclear receptor.

* Corresponding author. Tel.: +81 92 642 2585; fax: +81 92 642 2607.
E-mail address: nosescc@chem.kyushu-univ.jp (T. Nose).

0378-4274/$ – see front matter © 2009 Elsevier Ireland Ltd. All rights reserved.
doi:10.1016/j.toxlet.2009.08.001

tions carried out as part of the screening process have not always provided accurate results, primarily due to the lack of a good template for the docking calculation. Usually there is not much choice regarding template selection.

Human estrogen receptor α (hERα) is one of 48 NRs, and its ability to cause endocrine disruption has long been a source of concern. Fortunately, the X-ray crystal structures of hERα have been described for complexes with both agonists and antagonists. These prompted us to utilize computational analysis to forecast a compound that would fit the LBP of hERα by using the agonist-bound LBD and the antagonist-bound LBD as templates. In the present study, we carried out the docking and free energy calculations, and established a method called agonist/antagonist differential-docking screening (AADS). We used hERα-LBD crystal structures, two of which were originally coupled with agonists 17β-estradiol (E2) and diethylstilbestrol (DES), respectively, and another two with antagonists raloxifene (RAL) and 4-hydroxytamoxifen (4-OHT), respectively. We here report that the AADS method allowed us to identify 4-(1-adamantyl)phenol as a strong agonist of hERα.

2. Materials and methods

2.1. Materials

E2 and 4-(1-adamantyl)phenol (ADA) were purchased from Tokyo Kasei Kogyo Co., Ltd. (Tokyo, Japan), and 4-*n*-octylphenol (nOCT) was from Wako Pure Chemical Industries, Ltd. (Osaka, Japan). 4-*tert*-Octylphenol (tOCT) and 4-OHT were purchased from Sigma–Aldrich Co. (St. Louis, MO, USA). All other chemicals were of the best grade available.

2.2. Docking calculation by AutoDock

The automated docking method was applied to estimation of the appropriate complex structure between the test chemical and the ERα-LBD. Four different hERα-LBD three-dimensional (3D) structures were downloaded from the Protein Data Bank (PDB). These structures included 1ERE (A chain), 1ERR (A chain), 3ERD (A chain), and 3ERT (Brzozowski et al., 1997; Shiau et al., 1998). In order to prepare an appropriate receptor molecule for the docking calculation, missing hydrogen atoms were added in conjunction with the CHARMm force field by Discovery Studio 1.7 (Accelrys, San Diego, CA, USA). For this calculation, the bound ligands were removed from the 3D structures together with water molecules. All hydrogen atoms were energy-minimized using the minimization protocol of Discovery Studio (Adopted Basis NR, Max step = 2000, and Minimization RMS Gradient = 0.01). The vacant volumes of those LBDs were determined by means of the tool called the receptor–ligand interaction included in the Discovery Studio. As for antagonist-bound LBDs, the structural elements of the chemical, which are present outside of the LBP, were not involved in the vacant volume. The 3D structures of the test chemicals were prepared by Discovery Studio. The molecular volumes were also calculated by the Discovery Studio.

The docking calculation was performed using the AutoDock 3.0 software package running on a PowerMac G5 (Apple, Cupertino, CA, USA) to score ligand poses docked with a protein target (Morris et al., 1998). Polar hydrogen atoms were added, and Kollman united atom charges and atomic solvation parameters were assigned to the receptor molecule using AutoDock tools. Complete torsion of ligands was allowed to occur during docking. The grid maps representing the receptor molecule in the docking calculation were generated by the program AutoGrid. Each grid was centered at the LBP of hERα-LBD. The grid dimensions were large enough to cover the LBP and were 60 Å × 60 Å × 60 Å with a spacing of 0.375 Å between the grid points. The Lennard–Jones parameters 12-10 and 12-6, supplied with the program, were used for modeling H-bonds and van der Waals interactions, respectively. A Lamarckian genetic search algorithm was used for all docking calculations by AutoDock (Morris et al., 1998). The run parameters used in this study were as follows: the number of GA runs was 100, the maximum number of energy evaluations was 2.5×10^6, and the maximum number of generations was 1.0×10^5. Other parameters were represented by default values implemented by the program.

2.3. Estrogen receptor binding assay

The estrogen receptor binding assay using purified hERα-LBD was carried out by the previously reported method (Nakai et al., 1999). Varied concentrations (1×10^{-11} to 1×10^{-4} M) of sample solutions were mixed with the recombinant hERα-LBD, and the mixture solution was incubated for 1 h at 25 °C. After removal of free radioligands, radioactivity was determined on a liquid scintillation counter (TopCount NXT; PerkinElmer Life Sciences, Boston, MA, USA). The IC_{50} values (the concentrations for the half-maximal inhibition) were calculated from the dose–response curves obtained using the nonlinear analysis program ALLFIT (DeLean et al., 1978).

2.4. Luciferase reporter-gene assay

The reporter-gene assay was carried out essentially as described previously (Liu et al., 2007; Takayanagi et al., 2006). The ERα response element (ERE)-luciferase construct was generated and ligated into pGL3-Luc (Promega, Madison, WI, USA). Both the hERα expression and luciferase reporter plasmids were transiently transfected in HeLa cells, which were exposed to various concentrations of test chemicals to detect agonist activity. The antagonist activity was determined against E2.

3. Results and discussion

3.1. The docking screening of agonist E2 for the activation and inactivation conformations

The postulated procedure, the agonist/antagonist differential-docking screening (AADS) method, was first verified for known ligands of hERα. This procedure predicts the agonist or antagonist activity of small molecules from their binding energy, which is calculated by the docking program named AutoDock 3.0 in binding to a receptor with known 3D structure. We tested the ERα receptor structures determined as complexes with E2, DES, RAL, and 4-OHT (Fig. 1). These X-ray crystal structures are registered in PDB as 1ERE, 3ERD, 1ERR, and 3ERT, respectively. E2 and DES are agonists of hERα, while RAL and 4-OHT are antagonists.

In the present study, we first prepared the 3D structures of these compounds independently using the Discovery Studio computer program. The 3D structures of hERα with no ligand, namely 1ERE-desE2, 3ERD-desDES, 1ERR-desRAL, and 3ERT-des4-OHT, were utilized individually as templates for the docking calculations. Using the computer program AutoDock 3.0, the natural ligand E2 was evaluated for its ability to bind to the hERα-LBD templates. When E2 was docked with the template 1ERE-desE2, the complex afforded almost the same conformation as 1ERE itself. As shown in Fig. 2A, docked E2 (blue) is calculated to be located close to the native E2 (red). In these complexes, E2-phenol-hydroxyl group is hydrogen-bonded to Arg394 and Glu353. The program predicted the binding energy as −10.68 kcal/mol (Table 1).

When E2 was next docked with the template 3ERD-desDES, the complex also afforded a conformation similar to that of 1ERE (Orange, Fig. 2B). The E2-phenol-hydroxy group was hydrogen-bonded to Arg394 and Glu353 of hER-LBD derived from 3ERD-desDES. The binding energy for 3ERD-desDES was −10.90 kcal/mol (Table 1), which was somewhat smaller (ca. 0.22 kcal/mol) than that calculated for 1ERE-desE2. This difference is due to the water molecules, which are usually found in the LBP, being ignored in the docking calculation.

The structures of 1ERE and 3ERD represent the activation conformation induced by agonist binding, while those of 1ERR and 3ERT characterize the inactivation conformation with antagonist binding (Brzozowski et al., 1997; Shiau et al., 1998). When 1ERR-desRAL and 3ERT-des4-OHT were docked with E2, the binding energy was calculated to be −10.06 and −9.77 kcal/mol (Table 1). The results clearly show that the agonist E2 is much more stable in the activation conformation than in the inactivation conformation.

The average binding energy of E2 in the activation conformation was −10.79 kcal/mol (Table 1), while that in the inactivation conformation was −9.92 kcal/mol. The difference between these average energies was −0.87 kcal/mol, indicating that E2 is 0.87 kcal/mol more stable in the activation conformations 1ERE-desE2 and 3ERD-desDES than in the inactivation conformations 1ERR-desRAL and 3ERT-des4-OHT.

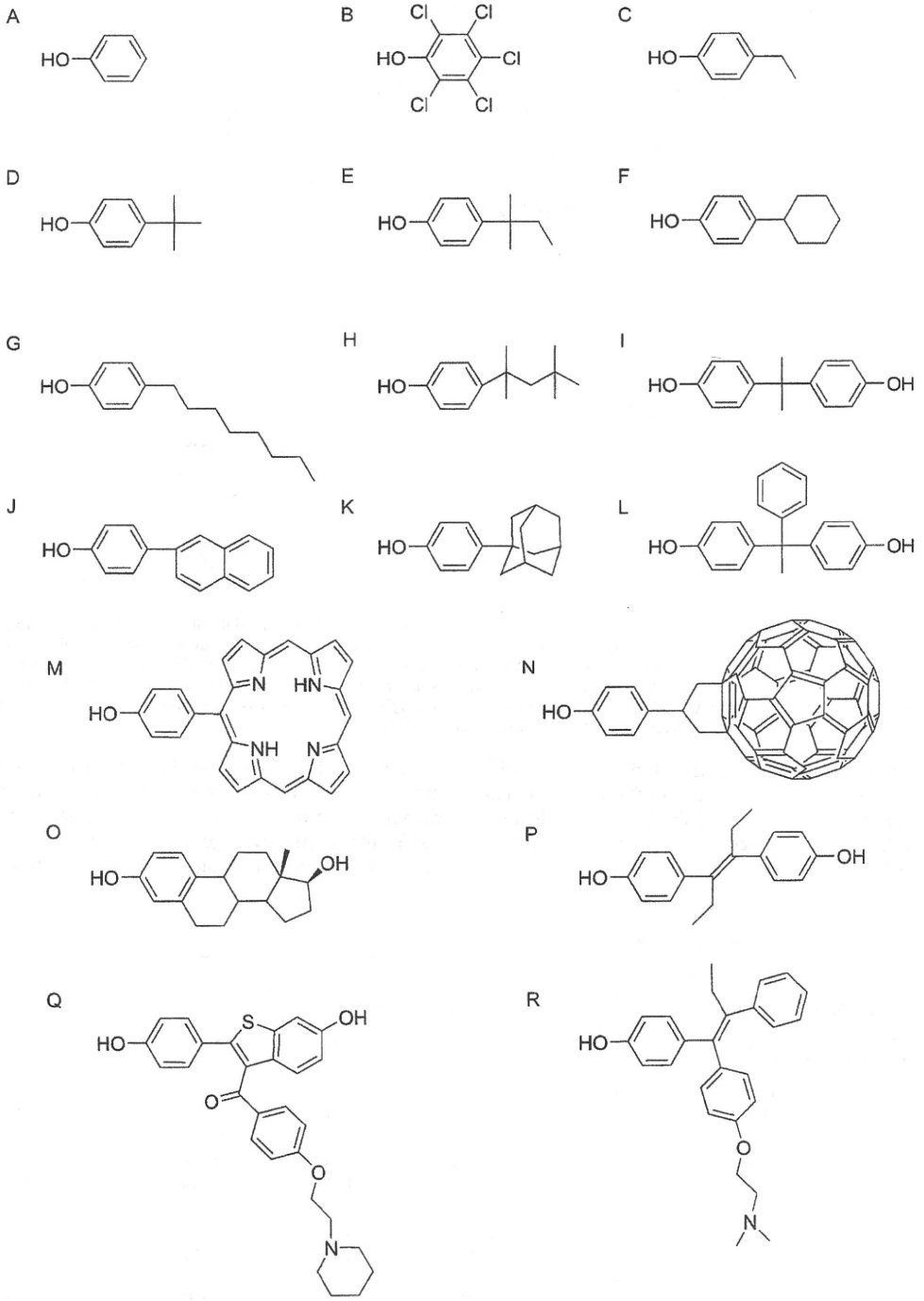

Fig. 1. Chemical structures of the phenol-related derivatives and ER-ligands used in this study. (A) Phenol, (B) pentachlorophenol (PCP), (C) 4-ethylphenol (ETP), (D) 4-*tert*-butylphenol (tBUT), (E) 4-*tert*-amylphenol (tAMY), (F) 4-cyclohexylphenol (CYC), (G) 4-*n*-octylphenol (nOCT), (H) 4-*tert*-octylphenol (tOCT), (I) bisphenol A (BPA), (J) 4-(2-naphthyl)phenol (NAP), (K) 4-(1-adamantyl)phenol (ADA), (L) bisphenol AP (BPAP), (M) 10-(4-hydroxyphenyl)porphyrin (POR), (N) C_{60}-conjugated phenol (C60), (O) 17β-estradiol (E2), (P) dietylstilbestrol (DES), (Q) raloxifene (RAL), and (R) 4-hydroxytamoxifen (4-OHT). Abbreviations of chemicals are denoted in parentheses.

3.2. Screening of DES, RAL, and 4-OHT for the activation and inactivation conformations

When DES was calculated for 1ERE-desE2 and 3ERD-desDES in the activation conformation, the binding energies were −8.95 and −9.39 kcal/mol, respectively (Table 1). The average binding energy was −9.17 kcal/mol. In contrast, those for 1ERR-desRAL and 3ERT-des4-OHT in the inactivation conformation were −8.66 and −8.91 kcal/mol, respectively, with the average binding energy being −8.79 kcal/mol (Table 1). It should be noted that −8.95 kcal/mol for 1ERE-desE2 and −8.91 kcal/mol for 3ERT-des4-OHT are almost equal to each other. The difference in the

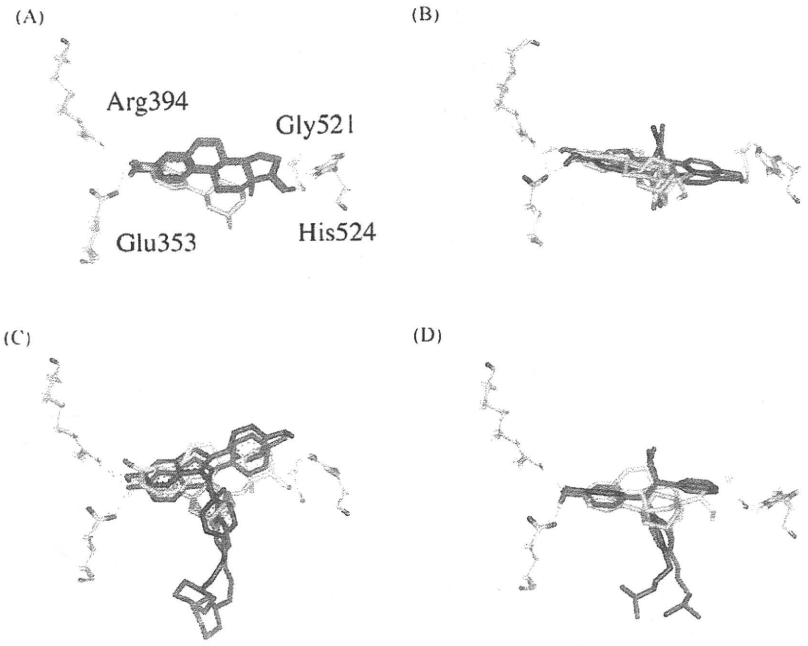

Fig. 2. Results of the docking calculations on four different ERα-LBDs. The docking templates used in this study were 1ERE-desE2 (A), 3ERD-desDES (B), 1ERR-desRAL (C), and 3ERT-des4-OHT (D), respectively. Amino acid residues (Arg394, Glu353, Gly521, and His524) that showed hydrogen-bonding (green lines) with docked ligands are shown. Ligands originally found in complexes, (A) E2, (B) DES, (C) RAL, and (D) 4-OHT, are depicted in red and the calculated ones in blue. Calculated E2 in the models (B), (C), and (D) is colored in orange. The root mean square deviation (RMSD) values of heavy atoms between the molecules calculated by AutoDock and the molecule determined by X-ray crystallography were as follows: (A) 0.74 Å, (B) 1.41 Å, (C) 1.47 Å, and (D) 1.65 Å. 4-(1-adamantyl)phenol is shown as a stick model with atomic color. (For interpretation of the references to color in this figure legend, the reader is referred to the web version of the article.)

average binding energies was −0.38 kcal/mol, indicating that DES is 0.38 kcal/mol more stable in the activation conformation than in the inactivation conformation. The partial similarity of molecular structures between DES and the antagonists RAL and 4-OHT might explain these results (Fig. 1).

Antagonists RAL and 4-OHT were also evaluated for their stability in the activation and inactivation conformations. RAL was demonstrated to be 0.79 kcal/mol more stable in the inactivation conformation (the average binding energy = −11.86 kcal/mol) than in the activation conformation (−11.07 kcal/mol) (Table 1). 4-OHT

Table 1
Docking of phenol derivatives and ER-ligands into the ERα-LBP.

Chemicals	Estimated free energy of binding (kcal/mol)						ΔG^a	$\Delta\Delta G^b$ (*Cpf*)[c]
	Agonist-bound receptor			Antagonist-bound receptor				
	1ERE	3ERD	Av.	1ERR	3ERT	Av.		
Agonist								
E2	−10.68	**−10.90**	−10.79	−10.06	−9.77	−9.92	−10.35	−0.87
DES	−8.95	**−9.39**	−9.17	−8.66	−8.91	−8.79	−8.98	−0.38
Antagonist								
RAL	−11.28	−10.86	−11.07	**−13.25**	−10.47	−11.86	−11.47	+0.79
4-OHT	−7.23	−8.50	−7.87	−10.54	**−10.77**	−10.66	−9.26	+2.79
Test chemicals								
Phenol	−4.16	**−4.54**	−4.35	−4.27	−4.18	−4.23	−4.29	−0.12
PCP	−6.13	**−6.48**	−6.31	−6.10	−5.33	−5.72	−6.01	−0.59
ETP	−4.99	**−5.29**	−5.14	N.D.	−4.75	−4.75	−4.95	−0.39
tBUT	−5.69	**−6.38**	−6.04	−5.55	N.D.	−5.55	−5.80	−0.49
tAMY	−5.86	**−6.53**	−6.20	−5.69	−5.57	−5.63	−5.92	−0.57
CYC	−6.93	**−7.27**	−7.10	−6.75	−6.48	−6.62	−6.86	−0.48
nOCT	−6.79	**−7.05**	−6.92	−6.77	−6.69	−6.73	−6.83	−0.19
tOCT	−7.45	**−7.91**	−7.68	−6.86	−6.77	−6.82	−7.25	−0.86
BPA	−7.37	**−7.45**	−7.41	−7.00	−7.10	−7.05	−7.23	−0.36
NAP	−7.63	**−8.25**	−7.94	−7.59	−7.30	−7.45	−7.69	−0.49
ADA	−8.96	**−9.50**	−9.23	−8.46	−8.43	−8.45	−8.84	−0.78
BPAP	**−8.10**	−7.02	−7.56	−7.85	−7.57	−7.71	−7.64	+0.15
POR	+5.27	+13.7	+9.49	**+4.05**	N.D.	+4.05	+7.68	−5.44
C60	>	>	-	>	>	-	>	-

N.D.: not determined. The docked chemical did not find in the LBP. Bold means the best score for each chemical in the four different calculations. -: not calculated; >: larger than +100 kcal/mol.

[a] ΔG: average of binding energies from four docking calculations.

[b] $\Delta\Delta G$: difference between average energies from the calculations used by agonist-bound receptor and antagonist-bound receptor.

[c] *Cpf*: conformation preference factor.

Table 2
Calculated molecular volume of ER-ligands and phenol derivatives.

Chemicals	Molecular volume (Å^3)	Relative volume (%)
Agonist		
E2 (17β-estradiol)	229.1	(100)
DES (diethylstilbestrol)	220.4	96.2
Antagonist		
4-OHT (4-hydroxytamoxifen)	319.9	140
RAL (raloxifene)	355.0	155
Test chemicals		
Phenol	75.7	33
PCP (pentachlorophenol)	155.3	67.8
ETP (4-ethylphenol)	104.4	45.6
tBUT (4-*tert*-butylphenol)	133.5	58.3
tAMY (4-*tert*-amylphenol)	148.0	64.6
CYC (4-cyclohexylphenol)	155.1	67.7
nOCT (4-*n*-octylphenol)	191.1	83.4
tOCT (4-*tert*-octylphenol)	191.5	83.6
BPA (bisphenol A)	187.6	81.9
NAP (4-(2-naphthyl)phenol)	176.2	76.9
ADA (4-(1-adamantyl)phenol)	198.7	86.7
BPAP (bisphenol AP)	235.2	103
POR (10-(4-hydroxyphenyl)porphyrin)	304.9	133
C60 (C_{60}-conjugated phenol)	581.6	254

Relative volume: molecular volume of E2 was used as the standard (100%).

was also judged to be 2.79 kcal/mol more stable in the inactivation conformation (−10.66 kcal/mol) than in the activation conformation (−7.87 kcal/mol) (Table 1). In conclusion, antagonists RAL and 4-OHT are more stable in the inactivation conformation.

The results for agonists E2 and DES show that they prefer to bind into the activation conformation of ERα-LBD. In contrast, the antagonists RAL and 4-OHT prefer the inactivation conformation. Such a feature for agonists or antagonists was also identified based on the best estimated free energy of binding score for each test chemical (Table 1). In addition to the four LBDs used here, if we could use the LBD structure, which best fits each test chemical, in the docking calculation, the calculation will provide the real best score to indicate both the binding potency and the biological activity of the chemical.

As to agonists and antagonists, what is the distinction between the two in hERα-LBDs? First, it was expected that the size of the LBPs must differ greatly, and the vacant volumes of the LBPs were found to vary considerably. The estimated volumes were 455 Å^3 for 1ERE-desE2, 339 Å^3 for 3ERD-desDES, 417 Å^3 for 1ERR-desRAL, and 468 Å^3 for 3ERT-des4-OHT. By contrast, the calculated molecular volumes of the ER-ligands were considerably different: 220–230 Å^3 for the agonists E2 and DES, while 320–355 Å^3 for the antagonists RAL and 4-OHT (Table 2). Antagonists are approximately 50% bigger than agonists.

3.3. *The agonist/antagonist differential-docking screening (AADS) method*

Agonists E2 and DES were found to be more stable in the activation conformation, while antagonists RAL and 4-OHT were more stable in the inactivation conformation. Antagonists (320–355 Å^3) were found to be approximately 50% bigger than agonists (220–230 Å^3). If these two issues, namely the suitable receptor conformation and the molecular size of chemicals, could be illustrated appropriately, differentiation between agonist and antagonist would become feasible. To this end, we defined the parameter as agonist/antagonist factor *Cpf* for the conformation preference.

Agonists prefer to bind the templates of agonist-bound LBD, and antagonists prefer to bind the templates of antagonist-bound LBD. Such preferences are thought to be a parameter to help identify the

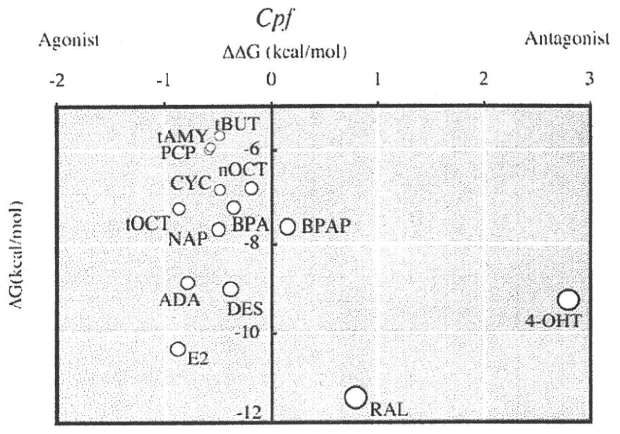

Fig. 3. Plotting analysis of the AADS method. ΔG versus $\Delta\Delta G$ plotting analysis. The agonist/antagonist factor ($\Delta\Delta G$) was calculated as the difference between average energies from each docking calculation used by agonist-bound receptor and antagonist-bound receptor. The size of each plot corresponds to the relative molecular size of the test chemical, as listed in Table 2.

biological activity of ligands. To set a parameter to determine the agonist/antagonist specificity, the factor ($Cpf = \Delta\Delta G$) was defined as follows:

$$Cpf = \Delta G(\text{activation conformation}) - \Delta G(\text{inactivation conformation}) \quad (1)$$

Here ΔG(activation conformation) is the average ΔG value from the docking calculations using agonist-bound hERα-LBD (1ERE and 3ERD) as templates. ΔG(inactivation conformation) is the average ΔG value from the docking calculations using antagonist-bound hERα-LBD (1ERR and 3ERT) as templates.

When the total average binding energy (ΔG) and agonist/antagonist factor ($Cpf = \Delta\Delta G$) of E2, DES, 4-OHT, and RAL were plotted (vertical, ΔG; horizontal, *Cpf*), it was clearly shown that the former two compounds, E2 and DES, are in the agonist area and the latter two, 4-OHT and RAL, are in the antagonist area (Fig. 3). It is clear that E2 is the best agonist with regard to both the binding energy and the agonist/antagonist preference. In contrast, among the antagonists, RAL exhibits the largest binding energy, while 4-OHT exhibits the biggest antagonist preference (Fig. 3). When the absolute values of agonist/antagonist factor were compared, 4-OHT exhibited the largest value and DES the smallest.

In the figure, the size of the molecules is indicated by their circle size (Fig. 3). It should be noted that the plots in the antagonists area are larger than those in the agonist area, indicating that ER-antagonists are much larger than the ER-agonists. We have called this line of analysis agonist/antagonist differential-docking screening (AADS). All the results obtained here imply that the AADS plotting analysis represents specific characteristics of chemicals, especially with regard to their reactivity to the nuclear receptor ER.

3.4. *The AADS method for test compounds*

In order to evaluate the ease of use of the AADS method, we tested a series of chemicals, 14 in total, as listed in Table 1. The average binding energies of the chemicals were obtained from the results of the docking calculations using four LBDs. Thus, the total average binding energy (ΔG) and the agonist/antagonist factor ($Cpf = \Delta\Delta G$) were estimated as in Table 1. The calculated free energies of binding (ΔG) of ER-ligands ranged from −4.29 to −8.84 kcal/mol. Apparently, the value for 10-(4-hydroxyphenyl)porphyrin (POR) cannot be corroborated because

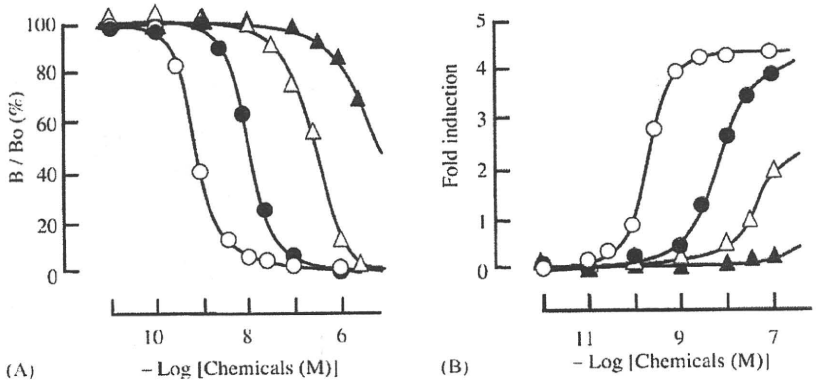

Fig. 4. Results of the binding assay and the reporter-gene assay. (A) Binding assay using purified hERα-LBD. (B) Reporter-gene assay. E2 (open circle), 4-(1-adamantyl)phenol (closed circle), 4-*tert*-octylphenol (open triangle), and 4-*n*-octylphenol (closed triangle). Data are presented as the mean from one representative experiment.

of its extreme instability in docking to any of the hERα-LBDs. This instability was further enhanced by C_{60}-conjugated phenol (C60), affording no convergent values (Table 1).

Among the 12 remaining compounds for which ΔG values were estimated, there was only one putative antagonist (Table 1 and Fig. 3). Because of its minus $\Delta\Delta G$ value, it is possible that BPAP has antagonist-like activity. However, as BPAP shows the best score against the agonist-form LBD, 1ERE, it may not work as an antagonist. On the other hand, we identified 4-(1-adamantyl)phenol (ADA) as a relatively strong agonist for hERα. ADA attained a binding energy (−8.84 kcal/mol) greater than that of the other test chemicals. The AADS method predicted that ADA is almost as active as DES (Table 1). In the calculated hERα-LBD–ADA complexes, the ADA-hydroxy group was found to form hydrogen bonds with Glu353 and Arg394 of hERα-LBD (Fig. 2). As shown in Fig. 3, ADA definitely excels with regard to both its binding energy and its agonist conformation preference.

3.5. Binding assay and reporter-gene assays for 4-(1-adamantyl)phenol (ADA)

By using the AADS calculation, 4-(1-adamantyl)phenol, ADA, was estimated as a putative ERα agonist. To confirm its binding and biological activities by other assays, we conducted the receptor binding assay and the luciferase reporter-gene assay. In the binding assay, ADA exhibited the most potent binding activity among the test chemicals used here, except for the known ERα-ligands, E2, DES, RAL, and 4-OHT (data not shown). Therefore, ADA was carefully tested in the binding and reporter-gene assays, and the results were compared with those for the agonist (E2), the antagonist (4-OHT), the weak ligand (*tert*-octylphenol), and the very weak ligand (*n*-octylphenol).

As shown in Fig. 4A, ADA showed a clear dose-dependent binding curve in the assay for hERα-LBD. Although ADA was approximately 60-fold weaker than the native agonist E2, its receptor binding activity (IC_{50} = 82.3 nM) was not as bad as a ligand of the receptor (Table 3). As a result, the prediction value of the AADS method was actually substantiated by the *in vitro* assay carried out to examine the receptor binding ability.

We next carried out the reporter-gene assay to determine the reporter activation potency of the chemicals. In this assay, ADA exhibited full agonist activity (Fig. 4B) as well as E2. When the concentration necessary to estimate full maximal activation, namely the EC_{50} value, was calculated, ADA exhibited significantly high activity at a concentration of 9.0 nM (Table 3). Indeed, ADA functioned as an agonist, as reported independently by Endo et al. (1999) for rat ERα. ADA is expected to be an excellent raw material for items such as nanoporous organosilicate thin films, and one should therefore be cautious with regard to its potential leakage (Cha et al., 2006). It is now clear that the AADS method can predict or foresee the activity of chemicals for human ERα by calculating the binding energy in the *in silico* docking modeling.

Table 3
Results of the competitive binding assay on ERα and biological activity through ERα activation by means of the luciferase reporter-gene assay of alkylphenols.

Chemicals	Binding assay IC_{50} (nM)	Reporter-gene assay EC_{50} (nM)
nOCT	N.D.	N.D.
tOCT	884 ± 175	33.3 ± 8.68
ADA	82.3 ± 12.4	9.00 ± 3.01
E2	1.40 ± 0.322	0.279 ± 0.035
4-OHT	0.720 ± 0.266	Inactive[a]

N.D.: not determined.
[a] 4-OHT exhibited antagonist activity in this assay.

tert-Octylphenol (tOCT) is a weak binder of hERα, while nOCT is almost completely inactive for hERα (Tabira et al., 1999). tOCT is intrinsically active in various biological assays, while nOCT is almost completely inactive in those assays (Miyawaki et al., 2008). Similar results were obtained in the present study, as shown in Fig. 4 and Table 3.

In conclusion, it should be noted that these results were well-predicted by the AADS method, as shown in Fig. 3. This procedure will provide a general method by using the LBD of each nuclear receptor as a template. It simultaneously provides the parameters of ΔG (binding potency) and *Cpf* ($\Delta\Delta G$, conformation preference factor), which can lead to prediction of the latent capabilities of EDCs.

Conflict of interest statement

None declared.

Acknowledgements

This work was supported in part by a Grant-in-Aid for Young Scientists (A) from the Ministry of Education, Culture, Sports, Science, and Technology of Japan, and Health and Labor Sciences Research Grants for Research on Risk of Chemical Substances from the Ministry of Health, Labor and Welfare of Japan.

References

Brzozowski, A.M., Pike, A.C., Dauter, Z., Hubbard, R.E., Bonn, T., Engstrom, O., Ohman, L., Greene, G.L., Gustafsson, J.A., Carlquist, M., 1997. Molecular basis of agonism and antagonism in the oestrogen receptor. Nature 389, 753–758.

Celik, L., Davey, J., Lund, D., Schiott, B., 2008. Exploring interactions of endocrine-disrupting compounds with different conformations of the human estrogen receptor alpha ligand binding domain: a molecular docking study. Chem. Res. Toxicol. 21, 2195–2206.

Cha, B.J., Kim, S., Char, K., Lee, J.-K., Yoon, D.Y., Rhee, H.-W., 2006. Nanoporous organosilicate thin films prepared with covalently bonded adamantylphenol pore generators. Chem. Mater. 18, 378–385.

Cui, J., Shen, X., Yan, Z., Zhao, H., Nagahama, Y., 2009. Homology-modeled ligand-binding domains of medaka estrogen receptors and androgen receptors: a model system for the study of reproduction. Biochem. Biophys. Res. Commun. 380, 115–121.

DeLean, A., Munson, P.J., Rodbard, D., 1978. Simultaneous analysis of families of sigmoidal curves: application to bioassay, radioligand assay, and physiological dose-response curves. Am. J. Physiol. 235, E97–102.

Endo, Y., Iijima, T., Yamakoshi, Y., Yamaguchi, M., Fukasawa, H., Shudo, K., 1999. Potent estrogenic agonists bearing dicarba-closo-dodecaborane as a hydrophobic pharmacophore. J. Med. Chem. 42, 1501–1504.

Fukuzawa, K., Kitaura, K., Nakata, K., Kaminuma, T., Nakano, T., 2003. Fragment molecular orbital study of the binding energy of ligands to the estrogen receptor. Pure Appl. Chem. 75, 2405–2410.

Fukuzawa, K., Kitaura, K., Uebayasi, M., Nakata, K., Kaminuma, T., Nakano, T., 2005. Ab initio quantum mechanical study of the binding energies of human estrogen receptor alpha with its ligands: an application of fragment molecular orbital method. J. Comput. Chem. 26, 1–10.

Germain, P., Staels, B., Dacquet, C., Spedding, M., Laudet, V., 2006. Overview of nomenclature of nuclear receptors. Pharmacol. Rev. 58, 685–704.

Heldring, N., Pike, A., Andersson, S., Matthews, J., Cheng, G., Hartman, J., Tujague, M., Strom, A., Treuter, E., Warner, M., Gustafsson, J.A., 2007. Estrogen receptors: how do they signal and what are their targets. Physiol. Rev. 87, 905–931.

Hong, H., Tong, W., Fang, H., Shi, L., Xie, Q., Wu, J., Perkins, R., Walker, J.D., Branham, W., Sheehan, D.M., 2002. Prediction of estrogen receptor binding for 58,000 chemicals using an integrated system of a tree-based model with structural alerts. Environ. Health Perspect. 110, 29–36.

István Virága, Tímea Polgárb, Keserub, G.M., 2005. Functional virtual screening of estrogen receptor alpha modulators by FlexX-Pharm. J. Mol. Struct. 725, 239–242.

Liu, X., Matsushima, A., Okada, H., Tokunaga, T., Isozaki, K., Shimohigashi, Y., 2007. Receptor binding characteristics of the endocrine disruptor bisphenol A for the human nuclear estrogen-related receptor gamma. Chief and corroborative hydrogen bonds of the bisphenol A phenol-hydroxyl group with Arg316 and Glu275 residues. FEBS J. 274, 6340–6351.

Miyawaki, J., Kamei, S., Sakayama, K., Yamamoto, H., Masuno, H., 2008. 4-tert-Octylphenol regulates the differentiation of C3H10T1/2 cells into osteoblast and adipocyte lineages. Toxicol. Sci. 102, 82–88.

Morris, G.M., Goodsell, D.S., Halliday, R.S., Huey, R., Hart, W.E., Belew, R.K., Olson, A.J., 1998. Automated docking using a Lamarckian genetic algorithm and an empirical binding free energy function. J. Comput. Chem. 19, 1639–1662.

Nakai, M., Tabira, Y., Asai, D., Yakabe, Y., Shimyozu, T., Noguchi, M., Takatsuki, M., Shimohigashi, Y., 1999. Binding characteristics of dialkyl phthalates for the estrogen receptor. Biochem. Biophys. Res. Commun. 254, 311–314.

Nose, T., Shimohigashi, Y., 2008. A docking modelling rationally predicts strong binding of bisphenol A to estrogen-related receptor gamma. Protein Pept. Lett. 15, 290–296.

Olefsky, J.M., 2001. Nuclear receptor minireview series. J. Biol. Chem. 276, 36863–36864.

Schmieder, P., Mekenyan, O., Bradbury, S., Veith, G., 2003. QSAR prioritization of chemical inventories for endocrine disruptor testing. Pure Appl. Chem. 75, 2389–2396.

Selassie, C.D., Garg, R., Mekapati, S., 2003. Mechanism-based QSAR approach to the study of the toxicity of endocrine active substances. Pure Appl. Chem. 75, 2363–2373.

Shiau, A.K., Barstad, D., Loria, P.M., Cheng, L., Kushner, P.J., Agard, D.A., Greene, G.L., 1998. The structural basis of estrogen receptor/coactivator recognition and the antagonism of this interaction by tamoxifen. Cell 95, 927–937.

Tabira, Y., Nakai, M., Asai, D., Yakabe, Y., Tahara, Y., Shinmyozu, T., Noguchi, M., Takatsuki, M., Shimohigashi, Y., 1999. Structural requirements of para-alkylphenols to bind to estrogen receptor. Eur. J. Biochem. 262, 240–245.

Takayanagi, S., Tokunaga, T., Liu, X., Okada, H., Matsushima, A., Shimohigashi, Y., 2006. Endocrine disruptor bisphenol A strongly binds to human estrogen-related receptor gamma (ERRgamma) with high constitutive activity. Toxicol. Lett. 167, 95–105.

J. Biochem. 2009;1–10
doi:10.1093/jb/mvp049

Placenta Expressing the Greatest Quantity of Bisphenol A Receptor ERRγ among the Human Reproductive Tissues: Predominant Expression of Type-1 ERRγ Isoform

Yukimasa Takeda[1,*], Xiaohui Liu[1], Miho Sumiyoshi[2], Ayami Matsushima[1], Miki Shimohigashi[2] and Yasuyuki Shimohigashi[1,†]

[1]Laboratory of Structure-Function Biochemistry, Department of Chemistry, The Research- Education Centre of Risk Science, Faculty of Sciences, Kyushu University, Fukuoka 812-8581; and [2]Division of Biology, Faculty of Science, Fukuoka University, Fukuoka 814-0180, Japan

Received February 19, 2009; accepted March 7, 2009; published online March 20, 2009

Estrogen-related receptor γ (ERRγ), one of the 48 human nuclear receptors, has a fully active conformation with no ligand. We recently demonstrated that ERRγ binds strongly bisphenol A (BPA), one of the nastiest endocrine disruptors, and thus retaining ERRγ's high basal constitutive activity. A report that BPA accumulates in the human maternal–fetal placental unit has led us to hypothesize that a large amount of ERRγ might exist in the human placenta. Here we report evidence that placenta indeed expresses ERRγ exceptionally strongly. We first ascertained the presence of nine different ERRγ mRNA variants and the resulting three ERRγ protein isoforms. By real-time PCR, we estimated the relative amount of ERRγ mRNA using total RNA extracts from human reproductive tissues. Placenta was found to express ERRγ extremely highly. Among the three ERRγ protein isoforms, placenta exclusively expresses the type-1 isoform, which possesses additional 23-mer amino-acid residues at the N-terminus of the ordinary ERRγ. This N-terminal elongation was found to elevate by approximately 50% the basal constitutive activity of ERRγ, as evidenced in the luciferase reporter gene assay. The present results suggest that BPA accumulates in the placenta by binding to ERRγ.

Key words: alternative splicing, bisphenol A receptor, estrogen-related receptor γ, placenta, real-time PCR.

Abbreviations: AR, androgen receptor; BPA, bisphenol A; ER, estrogen receptor; ERR, estrogen-related receptor; ERRE, ERR-response element; ERRγ, estrogen-related receptor γ; NRs, nuclear receptors; 4-OHT, 4-hydroxytamoxifen.

INTRODUCTION

Bisphenol A (BPA), 2,2-*bis*(4-hydroxyphenyl)-propane, is one of the highest volume chemicals produced worldwide as a starting material for polycarbonate plastics and epoxy resins. Long known as an estrogenic chemical, BPA is suspected of interacting with human estrogen receptor ER (*1*, *2*) or acting as an antagonist for a human androgen receptor (AR) (*3*, *4*). However, BPA's binding to ER and AR and its hormonal activity are extremely weak: 1,000–10,000 times weaker than with natural hormones.

Based on the idea that BPA may interact with nuclear receptors (NRs) other than ER and AR, we screened a series of nuclear receptors and eventually explored estrogen-related receptor γ (ERRγ) as the BPA target receptor. BPA was found to bind strongly to ERRγ with high constitutive basal activity (*5–7*). BPA's binding to ERRγ was further demonstrated by X-ray crystallographic analysis of the complex between BPA and ERRγ (*8*, *9*).

In our efforts to explore the genuine characteristics of ERRγ as a BPA receptor, we have noticed the presence of several different *ERRγ* mRNA isoforms. NRs often possess a number of mRNA isoforms produced by alternative splicing to exhibit functions in a tissue-specific or developmental stage-specific manner (*10*, *11*). However, little is known about the *in vivo* physiological functions of those splicing variants, and even the variants' tissue distributions are poorly understood.

BPA as an endocrine disruptor poses the worrisome threat of low-dose effects on reproductive and developmental processes in humans (*12*). To ensure the presence of *ERRγ* mRNA isoforms in human reproductive organs and brains, we attempted to quantify the total amount of *ERRγ* mRNAs and then the amount of each mRNA isoform. Here we report evidence that the human placenta expresses *ERRγ* mRNA extremely highly, and that the class of isoforms is type-1 ERRγ.

MATERIALS AND METHODS

cDNA Cloning—To confirm the presence of eight reported isoforms of *ERRγ* mRNA, we cloned cDNA by

*Present address: Cell Biology Section, Laboratory of Respiratory Biology, NIH-NIEHS, Research Triangle Park, NC 27709, USA.
†To whom correspondence should be addressed. Tel/Fax: +81-92-642-2584, E-mail: shimo@chem.kyushu-u.jp

using human pancreas and skeletal muscle. These total RNA samples (Clontech, Mountain View, CA, USA) were reverse-transcribed by using the forward primer of ERRγRT1 (5′-GAAAGCTGCTTCATAGTCTTGCTG-3′) and the enzyme SuperScriptII™ RNase H⁻ Reverse Transcriptase (Invitrogen, Carlsbad, CA, USA) at 42°C.

To confirm that all clones had inconsistent 5′-UTR sequences, the forward primers were designed separately, depending on the unique structure of each exon (Table 1). As reverse primers, ChERRγR1 and ChERRγR2 were used in the first and the nested PCRs, respectively. As for the amplification of *ERRγ1* cDNA, the first PCR was carried out using a primer set of ChERRγ1F/ChERRγR1 and the enzyme *Pfu Turbo*® Hotstart DNA Polymerase (Stratagene, La Jolla, CA, USA). The second PCR was performed by using PLATINUM® *Taq* DNA polymerase (Invitrogen) with another primer set of ChERRγ1F/ChERRγR2 and the product from the first PCR as a template. For amplification of all other *ERRγ*, PCR was carried out by the same method. Sequence analysis was carried out on CEQ8800 Genetic Analysis System (Beckman Coulter, Fullerton, CA, USA).

Real-Time PCR—The total RNA samples extracted from brains (adult and fetal) and various different reproductive tissues (ovary, uterus, placenta, prostate and testis) were purchased from Clontech, Stratagene and Biochain (Hayward, CA, USA). Each total RNA sample (1 μg) was reverse-transcribed by using SuperScriptII™ (Invitrogen) and oligonucleotide ERRγRT2 (5′-GGAGCAGTCATCATACAG-3′) and hgapdhRT (5′-ATGGTACATGACAA GGTG-3′).

Table 1. **The oligonucleotide sequences of primers used for cDNA cloning of a series of ERRγ mRNA isoform.**

Name of primers	Oligonucleotide sequences
Primers for amplification of ERRγ1 cDNA	
ChERRγ1F	5′-CTGTGCTCTGTCAAGGAAACTTTG-3′
ChERRγR1[a]	5′-GAAAGCTGCTTCATAGTCTTGCTG-3′
ChERRγR2[b]	5′-TTTCAACATGAAGGATGGGAAG-3′
Primers for amplification of ERRγ2 cDNA	
ChERRγ2F	5′-TACGCTAACACTGTCGCAGTTTG-3′
ChERRγ2-adF1	5′-GGTTTTGTAGACTTTCATAGCCAAAG-3′
ChERRγ2-adF2	5′-CGACTCACCTGATTAACCTGCTG-3′
ChERRγR1[a]	5′-GAAAGCTGCTTCATAGTCTTGCTG-3′
ChERRγR2[b]	5′-TTTCAACATGAAGGATGGGAAG-3′
Primers for amplification of ERRγ2-gig cDNA	
ChERRγ2-gigF1	5′-GCCACCACATCTCGATTCAAAG-3′
ChERRγ2-gigF2	5′-CACATGTTCGTGGTGTGGAAAG-3′
ChERRγR1[a]	5′-GAAAGCTGCTTCATAGTCTTGCTG-3′
ChERRγR2[b]	5′-TTTCAACATGAAGGATGGGAAG-3′
Primers for amplification of ERRγ3 cDNA	
ChERRγ3F1	5′-CGGTCCTTCACTTGGAGTTAGTG-3′
ChERRγ3F2	5′-CAAGCTTTATATAGGATCACCGTTGTG-3′
ChERRγR1[a]	5′-GAAAGCTGCTTCATAGTCTTGCTG-3′
ChERRγR2[b]	5′-TTTCAACATGAAGGATGGGAAG-3′
Primers for insertion/deletion confirmation of exon K	
ChERRγJF	5′-CAGAATGTCAAACAAAGATCGACAC-3′
ChERRγLR	5′-CAGCTGAGGGTTCAGGTATGG-3′

[a]The antisense reverse primer R1 has the same nucleotide sequence.
[b]The antisense reverse primer R2 has the same nucleotide sequence.

Real-time PCR was performed on a capillary-type LightCycler™ rapid thermal cycler system (Roche Diagnostics, Mannheim, Germany). Reactions were completed in a 10 μl solution mixture and SYBR Green Realtime PCR Master Mix (Toyobo, Tokyo). For normalization, the mRNA gene (*gapdh*) of the enzyme glyceraldehyde-phosphate dehydrogenase was amplified as an internal standard. The assay includes the steps of denaturation at 95°C for 1 min, annealing at 61°C for 3 s and extension at 72°C for a variable time, depending upon the size of products. The product specificity was always confirmed by agarose gel electrophoresis and routinely estimated by the melting curve analysis. To depict the standard curves for quantitative real-time PCR, a 10^{-1}-fold series of dilutions of each plasmid with the same DNA sequence was simultaneously amplified. Quantification of mRNA was achieved using LightCycler software (version 3.5). Standard curves had a correlation coefficient (r^2) of 1.00, linear over a sample concentration range, and mean square error values of 0.03–0.08 were involved.

Western Blotting Analyses—Western blotting was used to detect ERRγ protein isoforms from human kidney and placenta. ERRγ-specific mouse monoclonal antibody was purchased from Perseus Proteomics (Tokyo). The human placenta and kidney lysates were purchased from ProSci (Poway, CA, USA). These lysates (20 μg each) was electrophoresed on 10% polyacrylamide gels. After electrophoresis, gels were electro-blotted onto Hybond-P (GE Healthcare, Waukesha, WI, USA). The blot was incubated overnight in the presence of the anti-ERRγ monoclonal antibody. ERRγ protein was visualized by chemi-luminescence (GE Healthcare) using HRP-conjugated secondary antibody (Jackson ImmunoResearch, West Grove, PA, USA). To discriminate a positive band from negative ones, negative staining controls were performed without the first antibodies.

Reporter Gene Assay for ERRγ Types 1 and 2—Type I and type II ERRγ fragments were cloned into the vector pcDNA3.1(+) (Invitrogen). As an ERR response element (ERRE)-luciferase construct, 3 × ERRR/pGL3 was used as described previously (7). HeLa cells were maintained in Eagle's MEM medium (Nussui, Tokyo) with 10% (v/v) fetal bovine serum at 37°C. HeLa cells were transfected with 3 μg of luciferase reporter gene (pGL3/3 × ERRE), 1 μg of the expression plasmid of the wild-type of either type I or type II ERRγ and 10 ng pSEAP-control plasmid as an internal control by Lipofectamine Plus reagent (15 μl/ml, Invitrogen). Approximately 24 h after transfection, cells were harvested and plated into 96-well plates at a concentration of 5×10^4 cells/well. The cells were then treated with varying doses of chemicals, BPA (Tokyo Kasei Kogyo, Tokyo) and 4-OHT (Sigma-Aldrich, St. Louis, MO, USA), diluted with 1% BSA/PBS (v/v). After 24 h, luciferase activity was measured by using the Luciferase assay reagent (Promega, Madison, WI). SEAP activity was assayed by using Great EscAPe™ SEAP assay reagent (Clontech) according to the Fluorescent SEAP Assay protocol. Light emission was measured on a microplate reader Wallac 1420 ARVOsx (Perkin Elmer, Turku, Finland). Cells treated with 1% BSA/PBS were

used as a vehicle control. Each assay was performed in duplicate and repeated at least three times.

RESULTS

Confirmation and Classification of Alternative Splicings of ERRγ Gene—To date, three independent investigations have revealed six alternative splicing sites for the human *ERRγ* mRNA gene and eight different *ERRγ* mRNA variants (*13–15*). However, there is no systematic study to unify these results, and thus it is unclear whether or not all of these variants are present simultaneously in one species, such as humans. Thus, we first attempted to confirm the full-length sequences of cDNAs derived from the eight *ERRγ* mRNA splicing variants.

To amplify each *ERRγ* mRNA isoform—*ERRγ1*, *ERRγ2*, *ERRγ2-gig* and *ERRγ3*—PCR was conducted successfully by using a series of forward sense and reverse antisense primer sets was designed for each isoform (Table 1) and commercially available pancreas and skeletal muscle cDNAs. As a result, seven of the eight splice variants reported were definitely identified, but we could not identify *ERRγ3* in this study. Although we carefully searched many other human tissues, the mRNA corresponding to *ERRγ3* was not detected. Instead, we identified another novel variant *ERRγ2-bcd* (accession number AB362218). It should be noted that these variants have variable nucleotide sequences of the 5′-UTR, with no structural changes of ERRγ2 protein.

We now know nine splicing variants in total. It should be noted, however, that these variants afford or produce three distinctly different protein isoforms (Fig. 1), as the variants are classified into three mRNA isoforms: *ERRγ1*, *ERRγ2* and *ERRγ3*. Here, type-2 mRNA *ERRγ2* consists of seven subclasses of splicing variants: *ERRγ2-df*, *ERRγ2-def*, *ERRγ2-di*, *ERRγ2-d*, *ERRγ2-ad*, *ERRγ2-bcd* and *ERRγ2-gig* (Fig. 1C), although all of these variants produce the same receptor protein molecule of ERRγ2. The variants are constituted from 15 distinct exons, A–O, coded in the human genomic DNA in the very broad region of chromosome 1 (about 1,000 kbp) (Fig. 1B). The heterogeneity at the 5′-UTR is due to the presence of alternative transcription start sites and alternative splicing sites.

The type-1 protein isoform ERRγ1 has an additional 23-mer elongated N-terminal sequence. Type-2 mRNA genes, *ERRγ2* isoforms, include six variants containing the exon D-based fragment (designated *d*) in the 5′UTR. *ERRγ2-ad*, where *ad* indicates that the exons *a* and *d* are involved in this order, was first isolated from the human fetal brain library by Eudy *et al.* (*13*). On the other hand, *ERRγ2-gig* has been found only in the skeletal muscle cDNA library (*14*). The mRNA *ERRγ3-bcf* gene producing ERRγ3 has recently been reported by Kojo *et al.* (*15*), although we could not identify this gene in the present study. The ERRγ3 protein isoform has a deletion of 39-mer amino-acid residues in the DNA-binding domain of ERRγ2, resulting in an incomplete construction of the DNA binding site. In addition, it was found that *ERRγ* mRNAs each have two alternative polyadenylation isoforms (*13*).

Quantitative Analysis of ERRγ mRNA Genes as a Whole by Real-Time PCR—By means of real-time PCR, the total expression amount of the human *ERRγ* mRNA genes was estimated to amplify the region common to all the splicing variants. We designated the *hERRγ-whole* mRNA segment. We did confirm that there is no contamination of the genomic DNA in these RNA samples, since we could not amplify any cDNA when we used the primer sets directly for the samples.

To analyse the *hERRγ-whole* mRNA gene by real-time PCR, the primer set of sense hERRγwholeF and antisense hERRγwholeR was utilized (Table 2). For the quantification of each *ERRγ* splicing variant, real-time PCR was carried out by using a series of primer sets

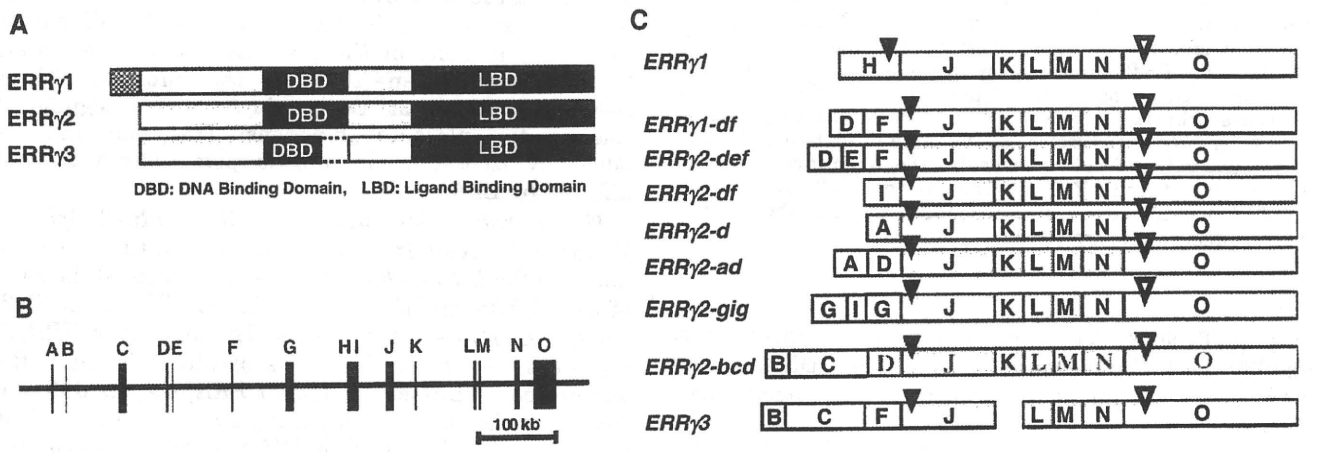

Fig. 1. **Structural constitution of *ERRγ* mRNA isoforms and ERRγ protein isoforms.** (A) Structure of ERRγ protein isoforms. ERRγ1 has 23-mer amino-acid extension at the N-terminus of ordinary ERRγ, namely ERRγ2. ERRγ3 has a 39-mer amino-acid deletion in the DNA binding domain. (B) Structural constitution of exon and intron of human *ERRγ* genomic gene. Alphabetic letters A–O each indicate an independent exon. (C) Structural constitution of exons in nine *ERRγ* mRNA isoforms. Closed arrowheads indicate the position of an AUG initiation codon, and open arrowheads indicate the position of a termination codon in the ERRγ open reading frame.

Table 2. **The nucleotide sequences of the primers used for the quantification of whole ERRγ mRNA and each ERRγ mRNA isoform.**

Name of primers	Oligonucleotide sequences	Length of products (bp)
Primers for quantification of ERRγ-whole mRNA		
hERRγwholeF	5′-CAGAATGTCAAACAAAGATCGACAC-3′	148
hERRγwholeR[a]	5′-GGTTGAACTGTAGCTCCCACTG-3′	
Primers for quantification of ERRγ1 mRNA		
hERRγ1F	5′-GCACATGGATTCGGTAGAACTTTG-3′	215
hERRγ1R[a]	5′-GGTTGAACTGTAGCTCCCACTG-3′	
Primers for quantification of ERRγ2 mRNA		
hERRγ2F	5′-TACGCTAACACTGTCGCAGTTTG-3′	183, 300, 338, 359[b]
hERRγ2R[a]	5′-GGTTGAACTGTAGCTCCCACTG-3′	
Primers for quantification of ERRγ2-gig mRNA		
hERRγ2-gigF	5′-GCCACCACATCTCGATTCAAAG-3′	339
hERRγ2-gigR[a]	5′-GGTTGAACTGTAGCTCCCACTG-3′	
Primers for quantification of ERRγ2-bcd Mrna		
hERRγ2-bcdF	5′-GATGTTGCTACACGGTCCTTCAC-3′	208
hERRγ2-bcdR	5′-TGATCTTCTGCAAAGACCCTACTTC-3′	
Primers for quantification of gapdh mRNA		
hgapdhF	5′-CAGCAAGAGCACAAGAGGAAGA-3′	107
hgapdhR	5′-GTCTACATGGCAACTGTGAGGAG-3′	

[a]These antisense primers have the same nucleotide sequence. [b]The number of products depends on the number of alternative splicing sites in the particular region amplified.

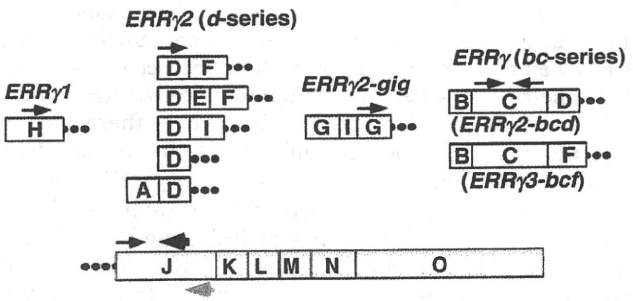

Fig. 2. **Design strategy of forward sense and reverse antisense primers for real-time PCR quantification of *ERRγ* mRNA isoforms.** Rightwards arrows indicate the forward sense primers, while leftwards arrows indicate the reverse antisense primers. Sense primers are specific to each mRNA isoform. For *ERRγ2* containing exon D, *ERRγ2-df*, *def*, *di*, *d*, *ad* and *bcd* the same sense primer was set in exon D (Table 2). For *ERRγ2-bcd* isoforms, sense and antisense primers were set in the same exon, C. There are two different reverse antisense primers in exon J, besides the antisense primer in exon C for *ERRγ2-bcd* isoforms. The large black leftward arrow is a universal antisense primer for the quantification of all isoforms except for *ERRγ2-bcd*. The large grey leftward arrow is an *ERRγ*-specific antisense oligonucleotide for the reverse transcription to prepare cDNAs.

(Fig. 2, Table 2). These primers were designed not to amplify the *ERRγ* sequence on the genomic DNA, setting both sense and antisense primers in the independent exon region.

Real-time PCR was carried out at least three times for the cDNAs prepared from each total RNA sample of human adult kidney, placenta, ovary, uterus, prostate, testis and brain, as well as from the human fetal brain. We determined the number of molecules of the whole mRNA and respective mRNA isoforms, with 1×10^5 molecules of *gapdh* mRNA being the internal standard. For example, the molecular number of the *hERRγ-whole* mRNA of adult brain was 942 per 1×10^5 *gapdh* mRNA (Table 3). The fetal brain had 739 molecules (about 80% of the molecular number of adult brain).

In kidney, *hERRγ-whole* mRNA had a molecular number of 4,369, approximately 4.6-fold that of the adult brain (Table 3). Among the reproductive organ tissues, the placenta was found to express the highest number of *hERRγ-whole* mRNA molecule, 4,544, ~5% greater than that of kidney and thus about 5-fold that of the adult brain. This very high expression of *hERRγ* mRNA genes in the placenta was of course found to exceed those of other reproductive organs: 151 in ovary, 167 in uterus and 571 in testis (Fig. 3). The second highest amount was in the prostate (*1,637*) (Table 3). Thus, the amount in the placenta was approximately 3-fold greater than that in the prostate. These results suggest that ERRγ plays a very significant role in the placental functions. This may indicate adversely that the placenta is potentially the most affected by BPA.

Tissue Distribution Analysis of ERRγ mRNA Splicing Variants by Real-Time PCR—After real-time PCR to measure the *ERRγ-whole* mRNAs, we measured the ratio of each *ERRγ* mRNA isoform—*ERRγ1*, *ERRγ2*, *ERRγ2-gig* and *ERRγ3*—in the tissues. The amount of *ERRγ2-gig* needs to be estimated separately, because the forward sense primer specific for *ERRγ2-gig* is different from that for other *d*-containing *ERRγ2* isoforms. The approximate ratio of each mRNA isoform was calculated against the total number of copies of all mRNA isoforms. As a result, we could calculate the ratio of each *ERRγ* mRNA isoform among the total amount of *ERRγ-whole* mRNA (Table 3 and Fig. 4). Detailed data for these analyses are shown in the Table 4, in which donor

Table 3. **The results of real-time PCR quantification of *ERRγ-whole* mRNA and its subtypes in human tissues.**

Tissues	*ERRγ-whole* mRNA[a]	*ERRγ* mRNA isoforms (%)			
		Type-1	Type-2		
			d-series	*gig*	*bcd*[b]
Brain (adult)	942 ± 24	26.1 ± 9.5	73.5 ± 9.8	0.3 ± 0.2	0.1 ± 0.1
Brain (fetal)	739 ± 195	30.2 ± 11.6	68.8 ± 11.1	0.8 ± 0.6	0.2 ± 0.2
Kidney	4369 ± 1276	11.1 ± 2.8	88.4 ± 3.1	0.3 ± 0.2	0.2 ± 0.1
Pancreas	2742 ± 798	4.0 ± 0.3	94.7 ± 1.2	0.7 ± 0.7	0.6 ± 0.5
Skeletal muscle	247 ± 48	45.2 ± 18.3	7.1 ± 1.0	47.7 ± 18.1	0.0 ± 0.0
Placenta	4544 ± 1572	98.9 ± 0.7	1.1 ± 0.7	0.0 ± 0.0	0.0 ± 0.0
Prostate	1637 ± 217	20.2 ± 2.7	78.2 ± 3.4	1.4 ± 0.6	0.2 ± 0.2
Testis	571 ± 93	23.6 ± 1.9	63.8 ± 1.6	11.0 ± 0.4	1.6 ± 1.1
Ovary	151 ± 50	18.0 ± 4.1	76.2 ± 8.1	3.5 ± 3.5	2.3 ± 2.2
Uterus	167 ± 127	4.3 ± 2.3	93.1 ± 3.7	2.6 ± 2.6	0.0 ± 0.0

[a]The amount of mRNA was calculated as the number of molecules per 1.0×10^5 *gapdh* mRNA molecules. [b]The analysis with specific sense and antisense primers, both of which were set in the same exon C (Fig. 2) was originally designed to measure the total amount of *c*-containing *ERR* mRNAs including *ERRγ2-bcd* and *ERRγ3-bcf*. Since the amount of *ERRγ3-bcf* that gives ERRγ3 was negligible, the measurement gave the amount of only *ERRγ2-bcd* that affords ERRγ2.

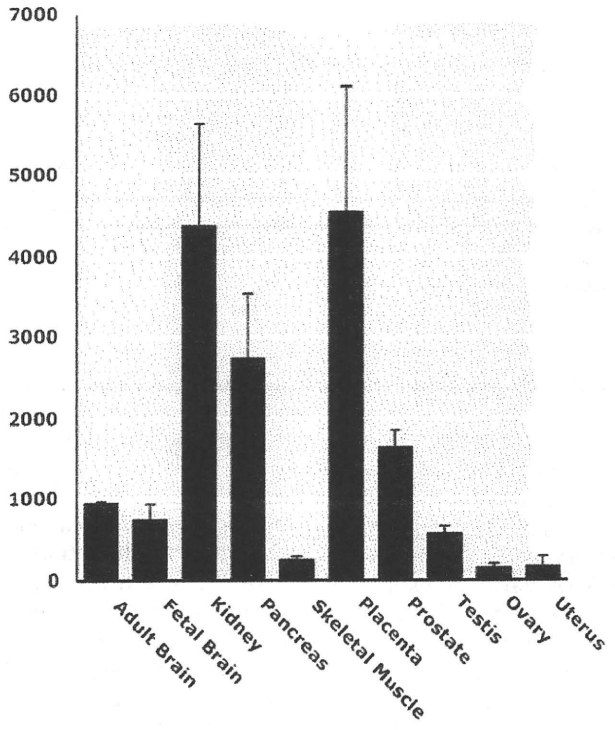

Fig. 3. **Quantitative real-time PCR for estimation of *ERRγ* mRNA expression in human brains and reproductive organs.** The *gapdh* mRNA gene was used as an internal control. The copy number per 1×10^5 *gapdh* mRNA was estimated for *ERRγ-whole* mRNA in each tissue. The error bars indicate SEM.

information such as age and sex is given for samples provided from each agent.

It should be noted that in the placenta, the *ERRγ1* mRNA isoform is accounted for 98.9% of the quantity of all mRNA isoforms (Table 3). This predominance of the type-1 mRNA isoform is very surprising and unique among the human tissues. All other human tissues express *ERRγ2* as a major mRNA isoform. It is likely that ERRγ1 produced from the *ERRγ1* mRNA isoform may play a crucial and central role in the placenta.

Reproductive tissues other than placenta expressed the *ERRγ2* mRNA isoform much more than *ERRγ1*. The content of *ERRγ2* mRNA isoform was estimated as 79.6% in prostate, and 81.9% and 95.7% in ovary and uterus, respectively (Table 3). Since the expression level of *ERRγ2-gig* mRNA was almost negligible in these tissues (Table 4), estimated *ERRγ2* mRNA isoform includes exclusively six subclasses of splicing variants (*d*-series that contain: *ERRγ2-df*, *ERRγ2-def*, *ERRγ2-di*, *ERRγ2-d*, *ERRγ2-ad* and *ERRγ2-bcd*) (Fig. 1C). As for the testis, however, a prominent inconsistency was found. It contained about 11% of the *ERRγ2-gig* mRNA isoform. Furthermore, a discrepancy between the sum of all mRNA isoforms and the *ERRγ-whole* mRNA—the sum of total numbers of *ERRγ* mRNA isoform molecules was clearly smaller (by about 10%) than the total molecular number of *ERRγ-whole* mRNA (data not shown)—strongly suggested the presence of mRNA isoform(s) other than those measured.

The adult and fetal brains were found to have almost the same isoform constitutions (Table 3). The expression ratios of *ERRγ1* and *ERRγ2* mRNAs respectively were 30.2% and 69.8% in the fetal brain and 26.1% and 73.9% in the adult brain. Thus, brain is the tissue in which type-2 *ERRγ* mRNA is expressed predominantly. In kidney, the expression levels of *ERRγ1* and *ERRγ2* mRNAs were estimated to be approximately 11.1% and 88.9%, respectively. Pancreas was also one of the tissues in which type-2 *ERRγ* mRNA was expressed predominantly, 4.0% *ERRγ1* and 96.0% *ERRγ2*. The sum of *ERRγ1* and *ERRγ2* mRNAs occupied approximately 100% in these tissues.

The constitutional ratio of *ERRγ1*, *ERRγ2*(*d*-series) and *ERRγ2-gig* mRNAs in skeletal muscle was unique (Table 3). Their expression ratios were 45.2%, 7.1% and 47.7%, respectively. Skeletal muscle was found to be the tissue in which type-2 *ERRγ2-gig* mRNA is expressed very highly.

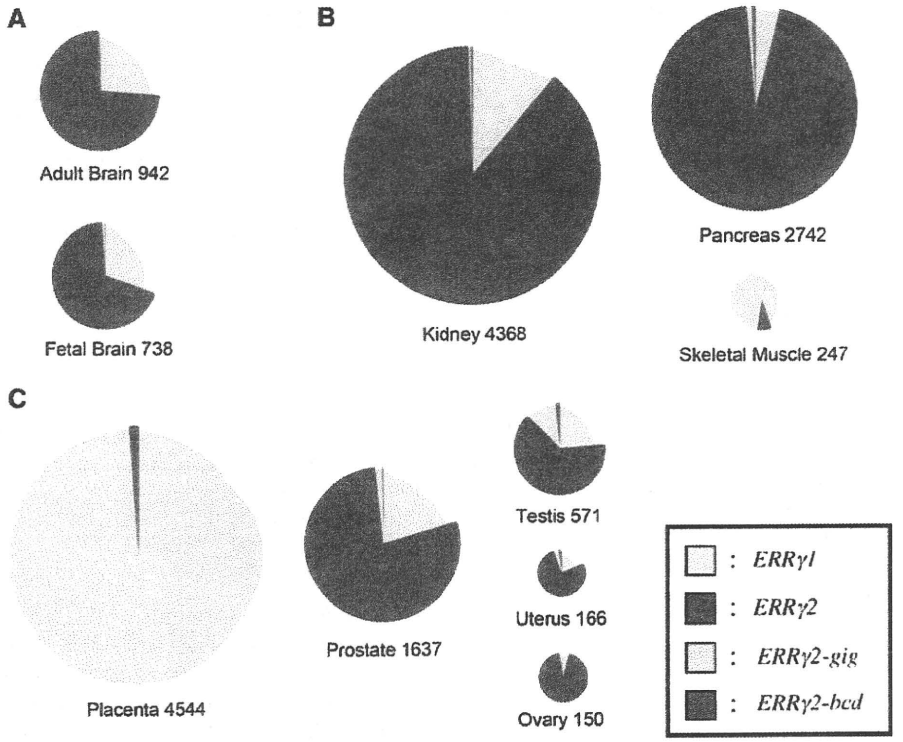

Fig. 4. **Quantitative real-time PCR for estimation of *ERRγ-whole* mRNA expression and percentage of the constitutions of *ERRγ* mRNA isoforms in human brains (A), standard tissues (kidney, pancreas and skeletal muscle) (B) and reproductive organs (C).** The circled area shows the total expression amount of *ERRγ-whole* mRNA in each tissue. The area of each color region in the circle is proportional to the expression amount of the *ERRγ* mRNA isoforms. Blue, purple, yellow and red areas indicate *ERRγ1*, *ERRγ2*(*d*-series), *ERRγ2-gig* and *ERRγ2-bcd* mRNA isoforms, respectively. The expression rates of each *ERRγ* mRNA isoform were calculated against the sum of the copy numbers of *ERRγ* mRNA isoforms.

In the estimation of the tissue distributions of *ERRγ* mRNA splicing variants, another important issue is to calculate the actual amount of each mRNA isoform. As shown in Fig. 4, *ERRγ1* mRNA isoform was most abundant in placenta, the amount of this isoform ($4,544 \times 98.9\%$ as in Table $3 = 4,494$ molecules) being exclusive and predominant. The kidney is the tissue in which the *ERRγ2* mRNA isoform is richest (3,884). Pancreas (2,632) and prostate (1,306) are also abounding in *ERRγ2*. As for the *ERRγ2-gig* mRNA isoform, skeletal muscle (118) and testis (63) contain it relatively highly.

Western Blotting Detection of ERRγ Protein Isoforms—To verify the amount of type-1 ERRγ protein isoform expressed in the placenta, Western blotting was carried out for the lysates of the human placenta and kidney. Kidney was selected as a reference because of its expected high expression (~90%) of the type-2 ERRγ protein isoform (see above). ERRγ protein isoforms were detected by using a monoclonal antibody specific for the N-terminal region (1–100) of ERRγ2, because this antibody can detect all three isoforms: ERRγ1, ERRγ2 and ERRγ3. The calculated molecular weight (51,313) of type-1 ERRγ is larger than that of type-2 standard ERRγ by ~2,700, apparently due to the N-terminal addition of 23-mer amino-acid residues.

The lysate isolated from kidney exhibited an intense protein band of 49 kDa, corresponding to the molecular weight of type-2 standard ERRγ. This band accompanied a faint band of 51 kDa, which corresponds to the molecular weight of type-1 ERRγ (Fig. 5). When we examined the lysate isolated from the placenta, the band of 51 kDa was markedly detected, as shown in Fig. 5. This result very clearly proves the consequences observed for the mRNA isoforms. It is evident that the mRNA variants expressed indeed produce a consequent protein and that the placenta expresses the type-1 ERRγ protein isoform predominantly and exclusively.

Transcription Activity of Type-1 and Type-2 ERRγ Isoforms in the Reporter Gene Assay—ERRγ is a constitutively active nuclear receptor that exhibits a high basal activity with no ligand. In the present study, we examined the reporter gene activity of type-1 and type-2 ERRγ isoforms by means of the luciferase reporter gene assay using HeLa cells. To normalize for transfection efficiency, we simultaneously carried out the SEAP assay (*16*). When the type-1 ERRγ isoform was compared with the type-2 standard ERRγ isoform, the constitutive activity level of type-1 ERRγ was found to be about 50% higher than that of type-2 ERRγ. As shown in Fig. 6, the type-2 ERRγ isoform exhibited significantly elevated constitutive activity (210% of the basal activity). Type-1 ERRγ isoform also exhibited considerably elevated constitutive activity (260%), a notably higher level than that of type-2. The results indicate that the N-terminal

Table 4. **Donor information for quantification of ERRγ-whole mRNA and its subtypes by quantitative real-time PCR.**

Tissues	Agent sources[a]	Age	Sex[b]	Number of donors	*ERRγ- whole* mRNA[c]	*ERRγ* mRNA isoforms (%)[d]			
						Type-1	Type-2		
							d-series	*gig*	*bcd*[e]
Brain	C	47–55	M	2	933	45.0	54.0	0.7	0.3
(adult)	S	66	F	1	906	18.1	81.9	0.0	0.0
	B	30	M	1	988	15.2	84.7	0.1	0.0
Brain	C	26–40[f]	M/F	21	555	15.5	82.1	1.9	0.5
(fetal)	S	19[f]	M	1	1128	53.2	46.8	0.0	0.0
	B	28[f]	F	1	533	21.9	77.4	0.6	0.1
Kidney	C	18–59	M/F	14	2540	16.5	82.4	0.7	0.4
	S	67	F	1	3742	7.2	92.7	0.0	0.1
	B	24	M	1	6824	9.7	90.2	0.0	0.1
Pancreas	C	35	M	1	4024	3.8	92.4	2.2	1.6
	S	72	M	1	1278	3.5	96.5	0.0	0.0
	B	44	M	1	2925	4.6	95.3	0.0	0.1
Skeletal	C	20–68	M/F	7	152	18.1	8.7	73.1	0.1
muscle	S	85	F	1	307	80.0	7.3	12.7	0.0
	B	87	F	1	283	37.3	5.4	57.3	0.0
Placenta	C	21–33	F	16	7538	99.6	0.3	0.1	0.0
	S	28	F	1	3880	99.5	0.5	0.0	0.0
	B	26	F	1	2214	97.6	2.4	0.0	0.0
Prostate	C	21–50	M	32	1420	22.8	74.8	2.0	0.4
	B	69	M	1	1854	17.5	81.6	0.9	0.0
Testis	C	24–64	M	39	693	21.7	62.9	11.7	3.7
	S	72	M	1	389	21.8	66.9	10.3	1.0
	B	27	M	1	632	27.3	61.7	11.0	0.0
Ovary	C	20–60	F	15	70	20.8	61.9	10.6	6.7
	S	49	F	1	139	10.0	90.0	0.0	0.0
	B	46	F	1	243	23.2	76.8	0.0	0.0
Uterus	C	40–61	F	3	70	4.9	87.3	7.8	0.0
	S	88	F	1	419	8.0	91.9	0.0	0.1
	B	49	F	1	11	0.0	100	0.0	0.0

[a]The samples of total RNA extracted from human tissues were purchased from Clontech (C), Stratagene (S) and BioChain (B). [b]M and F represent male and female, respectively. [c]The amount of mRNA was calculated as the number of molecules per 1.0×10^5 *gapdh* mRNA molecules. [d]The same antisense primer for *hERRγ-whole* mRNA was utilized for the quantification of *ERRγ1* and *ERRγ2* (Table 2). [e]The real-time PCR quantification to measure *c*-containing *ERR* mRNAs was carried out. Since the amount of *ERRγ3-bcf* was negligible, this counting was found to be just for *ERRγ2-bcd* that affords ERRγ2. [f]The age of fetal brain is shown by the number of weeks.

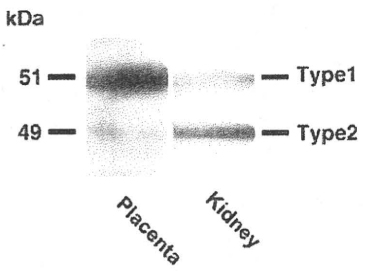

Fig. 5. **Western blotting analyses of ERRγ protein isoform expression levels.** An intense protein band of 49 kDa in kidney lysate corresponds to the molecular weight of type-2 standard ERRγ. The accompanying faint band of 51 kDa corresponds to the molecular weight of type-1 ERRγ. A major strong band of 51 kDa in the placenta lysate corresponds also to this type-1 ERRγ. Other bands are supposed to be specific or non-specific protein bands derived from the first antibody.

23-mer elongation has a distinct effect on the reporter gene transactivation activity of ERRγ.

4-OHT deactivated the ordinary standard type-2 ERRγ, as reported (*7*, *17*), diminishing the basal activity of ERRγ by up to 60–80% at a concentration of 10 μM (Fig. 7A). These were exactly revealed for the type-1 ERRγ isoform, ERRγ1. BPA, on the other hand, showed no effect on the basal constitutive activity of ERRγ even at a concentration of 10 μM, completely preserving ERRγ's high constitutive activity (Fig. 7A). The inverse agonist activity of 4-OHT for ERRγ1 was reversed or inhibited by BPA in a dose-dependent manner (Fig 7B). This reversing activity of BPA, namely, inverse antagonist activity of BPA, was revealed originally for the type-2 ERRγ isoform (*7*).

DISCUSSION

Extremely High Expression of ERRγ *mRNA in the Placenta*—In the present study, using commercially available human gene samples of reproductive organ

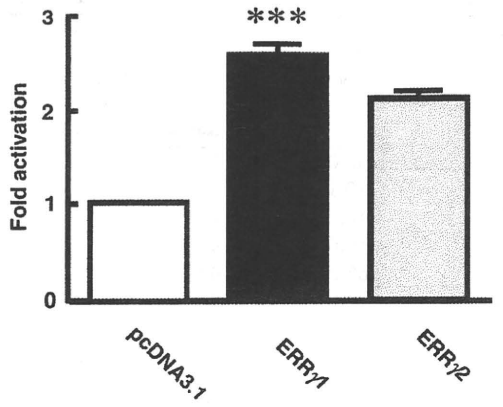

Fig. 6. **Transcription activity of type-1 and type-2 ERRγ isoforms in the reporter gene assay.** The type-1 ERRγ isoform is 23-mer larger than the type-2 ordinary ERRγ isoform at the N-terminus. HeLa cells were transfected with the luciferase reporter gene (3 × ERRE) and the expression plasmid of the wild-type of either type-1 or type-2 ERRγ. After 24 h, luciferase activity was measured. Cells treated with 1% BSA/PBS were used as a vehicle control. Each assay was performed in duplicate and repeated at least three times. To normalize the transfection efficiency, the SEAP assay, in which a second plasmid that constitutively expresses an activity that can be clearly differentiated from SEAP, was co-transfected simultaneously.

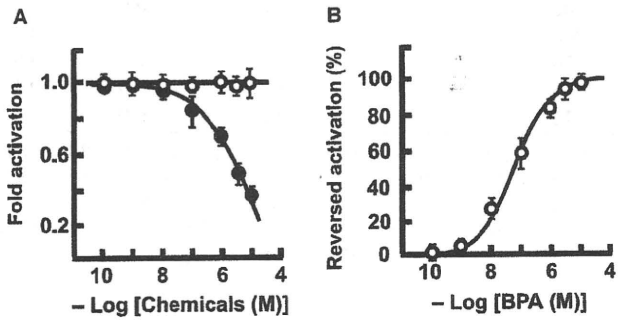

Fig. 7. **The luciferase reporter gene assay of BPA and 4-hydroxytamoxifen (4-OHT) for type-1 ERRγ.** (A) Deactivation of the fully activated human type-1 ERRγ isoform by the *inverse agonist* 4-hydroxytamoxifen (4-OHT) (filled circle) and sustainment by the *inverse antagonist* BPA (open circle). (B) Inverse antagonist activity of BPA (open circle) against the inverse agonist activity of 1.0 μM 4-OHT in ERRγ1. An amount of 1.0 μM 4-OHT exhibited ~0.4-fold deactivation, and the inverse antagonist activities are shown by the percentage of relative activity to reverse this deactivation activity. The high basal constitutive activity of type-1 ERRγ isoform was evaluated with the luciferase reporter plasmid (pGL3/3 × ERRE), and the highest activity was estimated in a cell preparation of 1.0×10^5 HeLa cells/well.

tissues and brains, we succeeded in the tissue distribution analyses of the *ERRγ-whole* mRNA gene and the constitutional ratios of a series of *ERRγ* mRNA isoforms. Real-time PCR for *whole-ERRγ* mRNA demonstrated an unexpectedly high expression of *ERRγ* mRNA in the placenta (Fig. 3). Western blotting also confirmed the expression of ERRγ protein (Fig. 5).

For accuracy in the quantification of *hERRγ-whole* mRNA, we repeated the real-time PCR. By using a new set of sense and antisense primers set at the 3′ terminal region, the results eventually obtained were almost the same as those of the first quantification shown in Fig. 3 (data not shown). For further confirmation, we tested internal controls other than *gapdh* mRNA. Those include the mRNA genes of human *β-actin*, *ubiquitin C*, *sdha* (succinate dehydrogenase complex, subunit A) and *hprt1* (hypoxanthine phosphoribosyl-transferase I). The results for the amount of *ERRγ* mRNA were almost the same as those obtained by the quantification using *gapdh* mRNA (data not shown). These further evidenced that the *ERRγ* mRNA expression in the human placenta is extreme, and the highest among the tissues examined.

Other reproductive organ tissues, such as ovary, uterus and testis, also express *ERRγ* mRNA, but at very low levels: 3.3%, 3.7% and 12.6% that of the placenta, respectively. Compared to these tissues, the considerably high expression of *ERRγ* mRNA in the prostate should be noted. The prostate had the second highest amount of *ERRγ* mRNA, approximately 36% of that in the placenta.

Predominant Expression of Type-1 Isoform of ERRγ *mRNA in the Placenta*—Nuclear receptors usually have several mRNA and protein isoforms by alternative splicing mechanisms, resulting in the exhibition of their functions in a tissue-specific or developmental stage-specific manner (*10*, *11*). Unfortunately, there is little understanding not only of the physiological functions of splicing variants, especially *in vivo*, but also of their tissue distributions in the majority of tissues throughout the body.

All transcript *ERRγ* mRNA variants consist of several distinct exons coded on human genomic DNA in the very broad region of chromosome 1 (about 1,000 kbp). As shown in Fig. 1B, the exons are thought to be distinguished between those in a variable region (A~I) and those in a consistent region (J~O). The latter includes almost all of the open reading frames of ERRγ, while 1–3 exons are selected from the variable region to form a 5′-UTR. Including alternative polyadenylation mechanisms, the gene expression of ERRγ appears to be severely regulated in a post-transcriptional manner. The sequence difference of the 5′-UTR should bring about a different translational efficiency, depending on the stability of mRNA produced and the presence of some upstream open reading frames (uORF) (*18*).

Type-1 ERRγ isoform (ERRγ1) has an additional 23-mer amino-acid residue extension at the N-terminus, and exhibits about 50% increased basal constitutive activity relative to that of ERRγ2 (Fig. 6). Although this isoform possesses exactly the same structure of its ligand-binding domain as other isoform types, its activation mechanism may differ from those of other isoforms by having this 23-mer N-terminal elongation. This might bring about unique tissue-specific function(s) in the placenta.

High Concentration of BPA in the Placenta due to High Expression of Type-1 ERRγ—BPA is an industrial chemical, and exposure to it is now widespread (*19*, *20*). We know now that BPA binds to ERRγ about 100 times greater than to ERα and ERβ, and that BPA exhibits a distinct inhibition activity against 4-OHT in ERRγ.

In the present study, we did know that there are three isoforms possessing precisely the same ligand-binding domain (LBD). It should be noted that BPA can bind to all these ERRγ isoforms in any tissue.

This strongly suggests that the concentration of BPA in human tissues is directly proportional to the amount of ERRγ proteins. In our estimation in the present study involving reproductive organ tissues, the expression of *ERRγ* mRNA is largest in the placenta and second largest in the prostate. The BPA concentration in the placenta has been reported to be approximately five times higher than that in maternal and fetal plasma (*21*). It is now quite reasonable to believe that the high concentration of BPA is due to the large amount of ERRγ protein isoforms, almost entirely type 1, in the human placenta.

The Effects of BPA Accumulation or Binding to Type-1 ERRγ on Placental Functions—The placenta receives nutrients, oxygen, antibodies and hormones from the mother's blood and removes waste. It forms the placental barrier, which filters out some substances that could harm the fetus. However, some substances, including BPA and viruses, are not filtered out, suggesting that the placenta does not act as a barrier against BPA (*21*, *22*). In addition to transferring gases and nutrients, the placenta also has metabolic and endocrine activity. It produces estrogen, relaxin, and human chorionic gonadotrophin, progesterone and somatomammotropin, all of which are important in maintaining pregnancy and the large amounts of glucose and lipids in the maternal blood. It is now evident that the placenta expresses BPA receptor ERRγ very highly. What would happen with the accumulation of BPA in the placenta?

Placentation in BPA-administered mice during pregnancy was reported to be abnormal (*23*), directly decreasing the number of embryos. In addition, almost all mouse neonates exposed to BPA were dead within 3 days after birth. Thus, BPA might disrupt the placental functions directly or indirectly, and might affect the mortality of neonates through indirect exposure of embryos. These are likely mediated through the BPA receptor ERRγs, at least in part. BPA administration has also been reported to significantly increase the weight of the uterus and the number and fertilization quality of sperm (*24*). DNA microarray analysis has shown that BPA administration increases the mRNAs of some nuclear receptors in mouse placenta (*25*). These results suggest that BPA affects the transcriptional regulation in the placenta or other reproductive organs through certain particular transcription factors.

Based on the fact that BPA strongly binds to ERRγ, the abnormality and probable change of gene expression in the placenta are likely accompanied by BPA binding to ERRγ. In this study, we demonstrated that the *ERRγ1* mRNA gene expresses almost fully in the placenta, and that the resulting type-1 ERRγ receptor is noticeably more potent than the resulting type-2 ERRγ receptor that expresses dominantly in other tissues. BPA would sustain unnecessarily this very high basal constitutional activity of type-1 ERRγ receptor in the placenta.

Other Human Tissues with High Expression of ERRγ *mRNA*—Adult and fetal brains, kidney and pancreas were the tissues in which ERRγ expresses significantly and considerably highly. In these tissues, type-2 *ERRγ* mRNA is expressed predominantly, while the expression levels of *ERRγ3* is almost negligible. The expression ratios of *ERRγ1* and *ERRγ2* mRNAs respectively varied 4–30% and 69–95%. As compared to the type-2 ERRγ isoform (ERRγ2), type-1 isoform ERRγ1 has an additional 23-mer amino-acid elongation at the N-terminus. Although ERRγ1 exhibits about 50% increased basal constitutive activity relative to that of ERRγ2 (see above), physiological functions in these tissues have never been clarified nor analysed for both ERRγ1 and ERRγ2.

As for the prostate, the mRNA gene was for the most part (~80%) *ERRγ2*. Various effects of estrogenic chemicals including BPA have been reported for the prostate. For example, acceleration in the proliferation rate of prostate epithelium during fetal life was noted to disrupt permanently the cellular control systems and to predispose the prostate to disease in adulthood (*26*, *27*). The effects of estrogens on the prostate, or the effects of their involvement in prostate cancer development and benign prostatic hyperplasia, are likely mediated through their ERs. In addition to the androgen receptor, which plays a central role in the normal development and neoplastic growth of the prostate gland, estrogens have long been suggested to play synergetic or distinct roles in the same processes. However, studies from ER knockout mouse models have shown neither ERα nor ERβ affects the targeted disruption of prostatic phenotype and function (*28*). This strongly suggests the involvement of one or more nuclear receptors other than ER and that ERRγ is a probable candidate for involvement in prostatic growth and development. ERRγ might play regulatory roles in normal and neoplastic prostatic cells by sharing similar ER-mediated pathways or acting independently.

CONCLUSION

The present study provides a valuable blueprint of ERRγ mRNA expression and important clues to understanding BPA's low-dose effects in humans. For instance, although the issue of bioavailability of parent BPA in humans has been contentious, the present results strongly suggest that the BPA concentration is proportional to the expression amount of ERRγ. There are scientific debates over whether or not low doses of BPA can have developmental or reproductive effects in humans. Now, it is clear that ERRγ, the receptor of BPA, abounds in brains and reproductive tissues such as the placenta and prostate.

Strong expression of ERRγ as a possible receptor of BPA in both the placenta and the fetal brain could have important implications for newborns. ERRγ is also a probable candidate for involvement in prostatic growth and development. However, the physiological roles of ERRγ are poorly understood at the moment. It is thus important to clarify such physiological functions and characteristics of ERRγ. Moreover, it is crucial to examine the content and extent of which BPA may influence these roles.

FUNDING

Health and Labour Sciences Research Grants for Research on the Risk of Chemical Substances, from the Ministry of Health, Labor and Welfare of Japan (to Y.S.); grants-in-aid from the Ministry of Education, Culture, Sports, Science and Technology of Japan (to Y.S.).

CONFLICT OF INTEREST

None declared.

REFERENCES

1. Krishnan, A.V., Stathis, P, Permuth, S.F., Tokes, L., and Feldman, D. (1993) Bisphenol-A: an estrogenic substance is released from polycarbonate flasks during autoclaving. *Endocrinology* **132**, 2279–2286
2. Olea, N., Pulgar, R., Perez, P., Olea-Serrano, F., Rivas, A., Novillo-Fertrell, A., Pedraza, V., Soto, A.M., and Sonnenschein, C. (1996) Estrogenicity of resin-based composites and sealants used in dentistry. *Environ. Health Perspect.* **104**, 298–305
3. Sohoni, P. and Sumpter, J.P. (1998) Several environmental oestrogens are also anti-androgens. *J. Endocrinol.* **158**, 327–339
4. Xu, L.C., Sun, H., Chen, J.F., Bian, Q., Qian, J, Song, L, and Wang, X.R. (2005) Evaluation of androgen receptor transcriptional activities of bisphenol A, octylphenol and nonylphenol *in vitro*. *Toxicology* **216**, 197–203
5. Okada, H., Tokunaga, T., Liu, X., Takayanagi, S., Matsushima, A., and Shimohigashi, Y. (2008) Direct evidence revealing structural elements essential for the high binding ability of bisphenol A to human estrogen-related receptor-γ. *Environ. Health Perspect.* **116**, 32–38
6. Liu, X., Matsushima, A., Okada, H., Tokunaga, T., Isozaki, K., and Shimohigashi, Y. (2007) Receptor binding characteristic of the endocrine disruptor bisphenol A for the human nuclear estrogen-related receptor γ. Chief and corroborative hydrogen bonds of the bisphenol A phenol-hydroxyl group with Arg316 and Glu275 residues. *FEBS J.* **274**, 6340–6351
7. Takayanagi, S., Tokunaga, T., Liu, X., Okada, H., Matsushima, A., and Shimohigashi, Y. (2006) Endocrine disruptor bisphenol A strongly binds to human estrogen-related receptor γ (ERRγ) with high constitutive activity. *Toxicol. Lett.* **167**, 95–105
8. Matsushima, A., Kakuta, Y., Teramoto, T., Koshiba, T., Liu, X., Okada, H., Tokunaga, T., Kawabata, S., Kimura, M., and Shimohigashi, Y. (2007) Structural evidence for endocrine disruptor bisphenol A binding to human nuclear receptor ERRγ. *J. Biochem.* **142**, 517–524
9. Matsushima, A., Teramoto, T., Okada, H., Liu, X., Tokunaga, T., Kakuta, Y., and Shimohigashi, Y. (2008) ERRγ tethers strongly bisphenol A and 4-α-cumylphenol in an induced-fit manner. *Biochem. Biophys. Res. Commun.* **373**, 408–413
10. Lu, N.Z. and Cidlowski, J.A. (2005) Translational regulatory mechanisms generate N-terminal glucocorticoid receptor isoforms with unique transcriptional target genes. *Mol. Cell* **18**, 331–342
11. Wang, Z., Zhang, X., Shen, P., Loggie, B.W., Chang, Y., and Deuel, T.F. (2006) A variant of estrogen receptor-α, hER-α36: Transduction of estrogen- and antiestrogen-dependent membrane-initiated mitogenic signaling. *Proc. Natl Acad. Sci. USA* **103**, 9063–9068
12. NTP-CERHR Monograph on the potential human reproductive developmental effects of bisphenol A (NIH Publication No. 08–5994; September 2008).
13. Eudy, J.D., Yao, S., Weston, M.D., Ma-Edmonds, M., Talmadge, C.B., Cheng, J.J., Kimberling, W.J., and Sumegi, J. (1998) Isolation of a gene encoding a novel member of the nuclear receptor superfamily from the critical region of Usher syndrom type IIa at 1q41. *Genomics* **50**, 382–384
14. Heard, D.J., Norby, P.L., Holloway, J., and Vissing, H. (2000) Human ERRγ, a third member of the estrogen receptor-related receptor (ERR) subfamily of orphan nuclear receptors: tissue-specific isoforms are expressed during development and in the adult. *Mol. Endocrinol.* **14**, 382–392
15. Kojo, H., Tajima, K., Fukagawa, M., Isogai, T., and Nishimura, S. (2006) A novel estrogen receptor-related protein γ splice variant lacking a DNA binding domain exon modulates transcriptional activity of a moderate range of nuclear receptors. *J. Steroid Biochem. Mol. Biol.* **98**, 181–192
16. Sambrook, J. and Russell, D.W. (2001) *Molecular Cloning: A Laboratory Manual* Cold Spring Harbor Laboratory Press, 3rd edn., Cold Spring Harbor, NY
17. Coward, P., Lee, D., Hull, M.V., and Lehmann, J.M. (2001) 4-Hydroxytamoxifen binds to and deactivates the estrogen-related receptor gamma. *Proc. Natl Acad. Sci. USA* **98**, 8880–8884
18. Meijer, H.A. and Thomas, A.A. (2002) Control of eukaryotic protein synthesis by upstream open reading frames in the 5'-untranslated region of an mRNA. *Biochem. J.* **367**, 1–11
19. vom Saal, F.S. (2006) Bisphenol A eliminates brain and behavior sex dimorphisms in mice: how low can you go? *Endocrinology* **147**, 3679–3680
20. Welshons, W.V., Nagel, S.C., and vom Saal, F.S. (2006) Large effects from small exposures. III. Endocrine mechanisms mediating effects of bisphenol A at levels of human exposure. *Endocrinology* **147**, S56–S69
21. Schonfelder, G., Wittfoht, W., Hopp, H., Talsness, C.E., Paul, M., and Chahoud, I. (2002) Parent bisphenol A accumulation in the human maternal-fetal-placental unit. *Environ. Health Perspect.* **110**, 703–707
22. Takahashi, O. and Oishi, S. (2000) Disposition of orally administered 2,2-bis(4-hydroxyphenyl)propane (bisphenol A) in pregnant rats and the placental transfer to fetuses. *Environ. Health Perspect.* **108**, 931–935
23. Tachibana, T, Wakimoto, Y, Nakamuta, N, Phichitraslip, T, Wakitani, S, Kusakabe, K., Hondo, E., and Kiso, Y. (2007) Effects of bisphenol A (BPA) on placentation and survival of the neonates in mice. *J. Reprod. Dev.* **53**, 509–514
24. Welshons, W.V., Thayer, K.A., Judy, B.M., Taylor, J.A., Curran, E.M., and vom Saal, F.S. (2003) Large effects from small exposures. I. Mechanisms for endocrine-disrupting chemicals with estrogenic activity. *Environ. Health Perspect.* **111**, 994–1006
25. Imanishi, S., Manabe, N., Nishizawa, H., Morita, M., Sugimoto, M., Iwahori, M., and Miyamoto, H. (2003) Effects of oral exposure of bisphenol A on mRNA expression of nuclear receptors in murine placental assessed by DNA microarray. *J. Reprod. Dev.* **49**, 329–336
26. Richter, C.A., Taylor, J.A., Ruhlen, R.L., Welshons, W.V., and vom Saal, F.S. (2007) Estradiol and bisphenol A stimulate androgen receptor and estrogen receptor gene expression in fetal mouse prostate mesenchyme cells. *Environ. Health Perspect.* **115**, 902–908
27. Timms, B.G., Howdeshell, K.L., Barton, L., Bradley, S., Richter, C.A., and vom Saal, F.S. (2005) Estrogenic chemicals in plastic and oral contraceptives disrupt development of the fetal mouse prostate and urethra. *Proc. Natl Acad. Sci. USA* **102**, 7014–7019
28. Jarred, R.A., McPherson, S.J., Bianco, J.J., Couse, J.F., Korach, K.S., and Risbridger, G.P. (2002) Prostate phenotypes in estrogen modulated transgenic mice. *Trends Endocrinol. Metab.* **13**, 163–168

Peptide Science 2008: M. Nomizu (Ed.)
The Japanese Peptide Society (2009)

ERα/ERRα Nuclear Receptor Heterodimer Directly Linked by A Flag Peptide

Shin Ikeda, Ayami Matsushima, and Yasuyuki Shimohigashi

Laboratory of Structure-Function Biochemistry, Department of Chemistry, Faculty and Graduate School of Sciences, Kyushu University, Fukuoka 812-8581, Japan
e-mail: sc208083@s.kyushu-u.ac.jp

It has recently been suggested that, in the tissues where both ERα and ERRα are present together, these nuclear receptors form a heterodimer to function specifically for characteristic physiological role with some efficacy. In the present study, we prepared expression vectors, which produce a recombinant protein of human ERα and ERRα cDNAs cross-linked directly with the FLAG peptide (DYKDDDDK). It was found that ERα in this heterodimer retains the ordinary characteristics of free ERα.

Keywords: estrogen receptor (ER), estrogen-related receptor (ERR), heterodimer, FLAG peptide, nuclear receptor

Introduction

Estrogen receptor α (ERα) and estrogen-related receptor α (ERRα) belong to steroid hormone receptors, or group III of nuclear receptor superfamily. These nuclear receptors function as a transcription factor, binding to their response element present in their target genes and facilitating their transcriptional role in the mRNA biosynthesis. ERRα binds to the ERR-response element (ERRE) as a monomer. ERRα also has an ability to form a homodimer for binding to functional estrogen response elements (EREs) in ER target genes. On the other hand, ERα can bind to ERRE *in vitro* as a dimer. These suggest that the transcriptional activation functions of ERRα and ERα must be overlapped *in vivo* [1].

There are some tissues where both ERα and ERRα are present together. In those tissues, ERα and ERRα have been suggested to form a heterodimer to function specifically for a certain characteristic physiological efficacy. In order to clarify such a dimer-specific effectiveness, it is essential to prepare a concrete heterodimer between ERα and ERRα in the cell nucleus. When they were merely co-expressed, homodimers of each ERα and ERRα would be produced simultaneously. Thus, in the present study, we prepared a gene construct bearing these two receptor proteins successively in a single chain.

Results and Discussion

Since the nuclear receptor protein biosynthesized should be transported from cytoplasm to nucleus to function as a transcription factor, it is necessary to ensure the synthesis of heterodimer and the transcriptional activity of each unit of nuclear